

AD-A107 748 NAVAL RESEARCH LAB WASHINGTON DC F/6 18/3
TRANSITION TO DOUBLE MACH STEM FOR NUCLEAR EXPLOSION AT 104 FT --ETC(U)
NOV 81 M FRY, J M PICONE, J P BORIS, D L BOOK
UNCLASSIFIED NRL-MR-4630 NL

NAVAL RESEARCH LAB WASHINGTON DC F/O 18/3
TRANSITION TO DOUBLE MACH STEM FOR NUCLEAR EXPLOSION AT 104 FT --ETC(U)
NOV 81 M FRY, J M PICONE, J P BORIS, D L BOOK
NRL-NR-4630 NL

UNCLASSIFIED

ML

4107748

END

DATE _____

FILMED

2

AD 4
LEVEL II

Transition to Double Mach Stem for Nuclear Explosion at 104 Ft Height of Burst

M. Fay

Science Applications, Inc.
McLean, VA 22102

J. M. PICONE, J. P. BORIS, AND D. L. BOOK

Laboratory for Computational Physics

November 17, 1981

This work was supported by the Defense Nuclear Agency under Subtask Y99QAXSG 0001, and work unit title "Flux-Corrected Transport."



NAVAL RESEARCH LABORATORY
Washington, D.C.

Approved for public release; distribution unlimited.

DTIC
ELECTE
NOV 25 1981
A

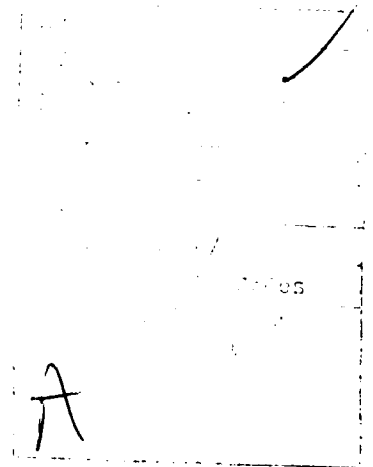
0111 25 022

FILE COPY

REPORT DOCUMENTATION PAGE		READ INSTRUCTIONS BEFORE COMPLETING FORM
1. REPORT NUMBER NRL Memorandum Report 4630	2. GOVT ACCESSION NO. AD-A107748	3. RECIPIENT'S CATALOG NUMBER
4. TITLE (and Subtitle) TRANSITION TO DOUBLE MACH STEM FOR NUCLEAR EXPLOSION AT 104 FT HEIGHT OF BURST		5. TYPE OF REPORT & PERIOD COVERED Interim report on a continuing NRL problem.
		6. PERFORMING ORG. REPORT NUMBER
7. AUTHOR(s) M. Fry*, J. M. Picone, J. P. Boris, and D. L. Book		8. CONTRACT OR GRANT NUMBER(s)
9. PERFORMING ORGANIZATION NAME AND ADDRESS Naval Research Laboratory Washington, DC 20375		10. PROGRAM ELEMENT, PROJECT, TASK AREA & WORK UNIT NUMBERS 44-0578-0-1
11. CONTROLLING OFFICE NAME AND ADDRESS Defense Nuclear Agency Washington, DC 20305		12. REPORT DATE November 17, 1981
		13. NUMBER OF PAGES 71
14. MONITORING AGENCY NAME & ADDRESS (if different from Controlling Office)		15. SECURITY CLASS. (of this report) UNCLASSIFIED
		15a. DECLASSIFICATION/DOWNGRADING SCHEDULE
16. DISTRIBUTION STATEMENT (of this Report) Approved for public release; distribution unlimited.		
17. DISTRIBUTION STATEMENT (of the abstract entered in Block 20, if different from Report)		
18. SUPPLEMENTARY NOTES *Present address: Science Applications, Inc., McLean, VA 22102 This work was supported by the Defense Nuclear Agency under Subtask Y99QAXSG, work unit 00001, and work unit title, "Flux-Corrected Transport."		
19. KEY WORDS (Continue on reverse side if necessary and identify by block number) Double Mach stem Height-of-burst (HOB) Flux-corrected transport (FCT) High-over-pressure		
20. ABSTRACT (Continue on reverse side if necessary and identify by block number) A nuclear height-of-burst (HOB) calculation has been performed using a two-dimensional flux- corrected transport (FCT) code. The calculation predicts the transition from regular to Mach reflection at ground ranges approximately equal to the HOB. The characteristics of the resulting waveforms are basically the same as those found in shock tube experiments when planar shocks reflect from wedges, and appear highly regular. In the double-Mach reflection region the first Mach stem is observed to toe out markedly compared with the planar case. In the high-over-pressure (regular reflection) region initialization errors and inadequate resolution caused pressure peaks to appear too low by about 20%. In the Mach reflection region the peak pressures are in good agreement with experimental data.		

CONTENTS

I. INTRODUCTION	1
II. DESIGN OF PROBLEM	4
III. COMPUTATIONAL DETAILS	6
IV. RESULTS AND PHENOMENOLOGY	9
V. SUMMARY	19
ACKNOWLEDGMENT	22
REFERENCES	23
APPENDIX A. DETAILED TIME HISTORY OF CALCULATION ...	24



TRANSITION TO DOUBLE MACH STEM FOR NUCLEAR EXPLOSION AT 104 FT HEIGHT OF BURST

I. INTRODUCTION

In a nuclear height-of-burst (HOB) detonation the spherical blast wave reflects from the ground, initially producing a regular reflection region. When the shock reaches a ground range approximately equal to the HOB an abrupt transition to Mach reflection occurs. This transition is responsible for an airblast environment more severe than the surface burst nuclear case. Qualitatively, it can be thought of as a partial flow stagnation in the Mach region that leads to the production of two static pressure peaks.

A 1 Kiloton (1 KT) atmospheric nuclear explosion at a HOB of 104 feet has been simulated using the two dimensional FAST2D code (Ref .1). Figure 1 illustrates the shock structure. The calculation predicts the transition of the shock from regular reflection to double Mach reflection. Because the spherical waves are expanding and thus decreasing in Mach number as well as angle of incidence with the ground, they create a dynamic Mach stem formation. In comparison to planar shocks on wedges one finds them to be qualitatively alike. The appearance of double peaks in the pressure and density profiles (versus time and distance) is interpreted as the point of transition. Other interesting phenomena such as the rollup of the contact surface generating a vortex ring and the associated phenomenon of toeing out of the first Mach stem can be observed.

The ability of the calculation to accurately predict the gasdynamic effects both temporally and spatially is due in part to the shock capturing and adaptive rezone features of the FAST2D code. A minimal number of very fine zones was placed around the shock front and these zones then moved with the first Mach stem to prevent shock smearing and distortion. This calculation is the first attempt to model the nuclear HOB case through the use of a Flux-Corrected Transport (FCT) algorithm (Ref. 2).

Manuscript submitted August 24, 1981.

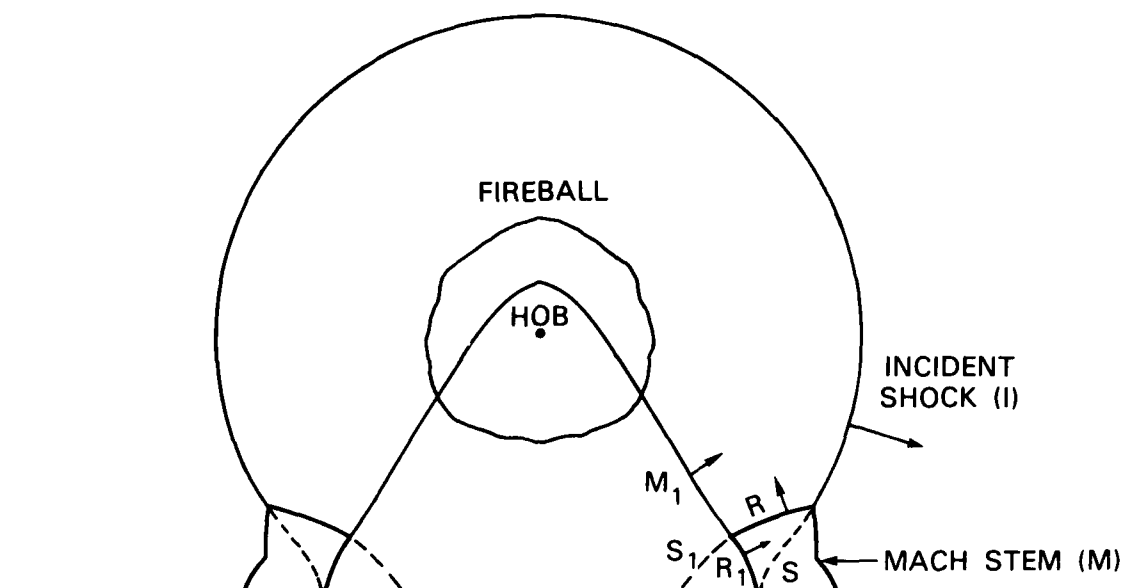


Fig. 1 - Mach stem structure from HOB

The results of this calculation agree well with the pressure-distance curve generated by the high explosive (HE) data of Carpenter (Ref. 3) and the analysis of Kuhl (Ref. 4). The peak overpressure of the first shock at the time of transition is about 4300 psi. Our simulation was run to 11.6 ms (total time with $t_0 = 3.76$ ms), which corresponds to pressure peaks of about 2000 psi. In the regular reflection region the peak values tend to be about 20% low due to the clipping of the FCT algorithm and inaccuracies in the initialization of the flow. Reducing the minimum zone size from 5 cm to 1 cm in a one-dimensional test calculation eliminated this discrepancy, however. In the two-peak regions the agreement between the experimental data and the values presented here is very good. The resolution of the calculation is adequate for studying qualitatively the characteristics of the flow field. For future work we recommend that the transition region be explored with improved resolution.

II. DESIGN OF PROBLEM

The problem of a 1-KT nuclear detonation at 104 ft (31.7m) HOB was chosen since it can be scaled conveniently to various HE tests. The use of the 1KT standard is also expedient; one could, however, have used realistic initial conditions, such as the Los Alamos Scientific Laboratory RADFLO or Air Force Weapons Laboratory (AFWL) SPUTTER calculations. A simple constant ambient atmosphere was used with a density of $1.22 \times 10^{-3} \text{ g/cm}^3$ and pressure $1.01 \times 10^6 \text{ dyne/cm}^2$. To relate the energy and mass densities to the pressure, a real-air equation of state (EOS) was used. This "table-lookup" EOS is derived from Gilmore's data (Ref. 5.) and has been vectorized for the TI Advanced Scientific Computer at NRL (Ref. 6). Figure 2 illustrates the effective gamma versus specific energy per unit mass for different values of the density. The internal energy density used in the call to the EOS is found by subtracting kinetic energy from the total energy; this can be negative due to phase errors in the fluid variables. When this occurs, the value of the pressure is reset to zero.

The transition from regular reflection to double Mach reflection is known to occur at a ground range approximately equal to the HOB. Therefore, the size of the mesh should be roughly twice the HOB in both directions. The upper boundary should be far enough away from the blast front to be noninterfering. We set the boundaries at $5.5 \times 10^3 \text{ cm}$ for the radial direction and $1.035 \times 10^4 \text{ cm}$ for the axial direction. The fine grid in the radial direction contained 140 out of 200 total zones, each 5 cm in length. The largest zones initially filled the right section of the grid and were 80 cm in length. A smoothing involving 40 zones was performed between the region to guarantee that the zone sizes varied slowly. In the vertical direction the fine grid contained 75 out of 150 total zones, each 5cm in length. Beyond that region the zones increased geometrically by a factor of 1.112.

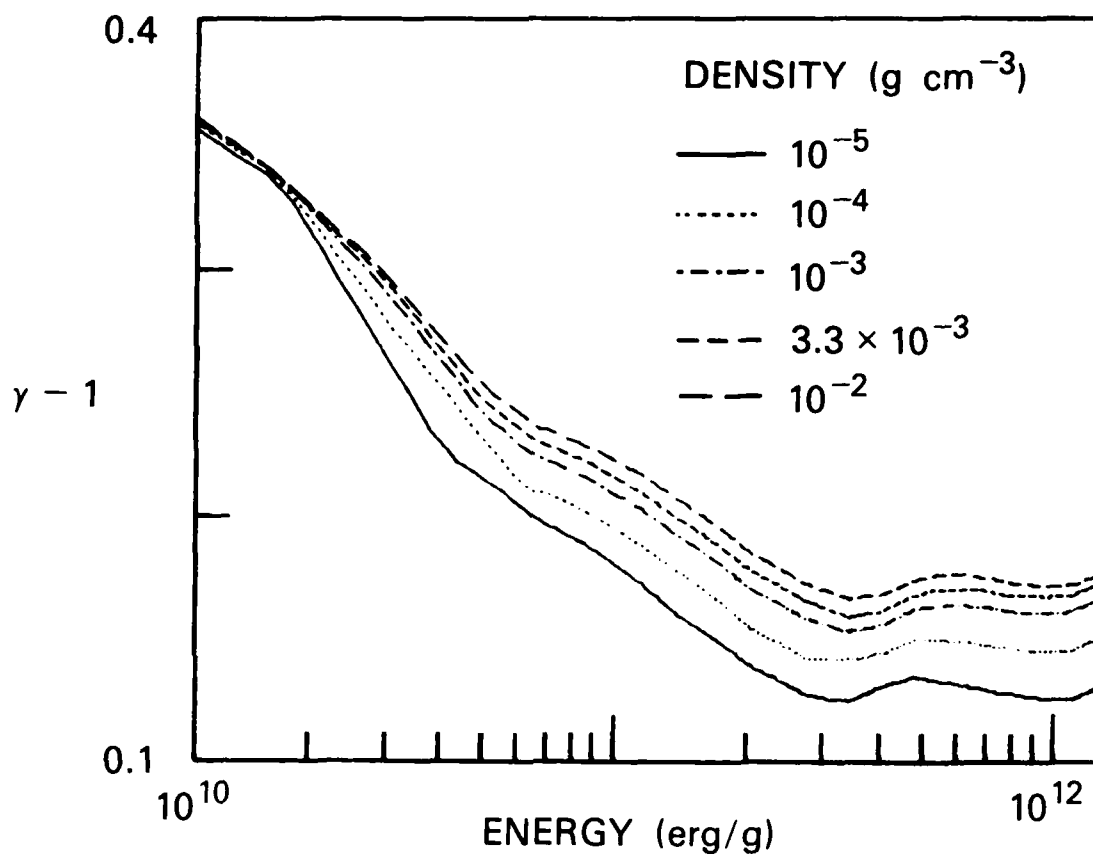


Fig. 2 - Gamma -1 vs. specific energy for Air EOS

Placement of the fine grid at the origin (ground zero - the point at which first reflection occurs) was determined to be optimum for capturing peak pressures in the airblast wave front. Thus, as the expanding wave moved along the ground surface, the fine grid was always locked to it, and each point along the incident blast front encountered the same spatial gridding as it approached the ground. By treating each point of the incident front in the same manner, we insured that the calculation was internally consistent and that the computed transition point was accurate to within the limits of the resolution. Finally, we point out that, as a section of the incident blast wave propagated within the fine grid, the wave steepened. The size of the fine grid was sufficient to insure that the incident wave had reached the maximum steepness prior to intersecting the ground.

The initialization provides a strong shock with Mach number $M_1 = 12$. This speed and the need for restart capability led to the choice of 200 timesteps as an interval for the spatial display ("snapshots"). The dump interval that resulted was $\sim \Delta t = 0.3$ milliseconds. These dumps were stored on magnetic tape and postprocessed.

Additional diagnostics were implemented in the calculation. Stations were created to gain information from fixed spatial positions within the calculational grid. These 25 physical variable sensors were placed along the ground and stored values of the energy and mass densities and velocity for every timestep. From this information one can construct static and dynamic pressure curves.

III. COMPUTATIONAL DETAILS

The evolution of the nuclear HOB flow field was modeled numerically with the FCT code FAST2D (Ref. 7). FCT yields accurate and well-resolved descriptions of shock wave propagation without the necessity of a priori knowledge of the essential gasdynamic discontinuities in the problem. Additionally, the code has a general adaptive regridding capability which permits fine zones to be concentrated in the region of greatest physical interest while the

remainder of the system is covered with coarse zones. Figure 3 depicts the grid setup initially and at transition to the double Mach stem structure. The rezone algorithm is programmed to track the Mach stem with the fine grid.

The transport algorithm used a low-phase-error phenical FCT algorithm in a model called JPBFACT, an advanced version of the ETBFCT algorithm described in Ref 1. The linear part of this algorithm is fourth-order accurate spatially in advection problems with a given constant velocity and has a (nonlinear) flux-corrected antidiffusion needed to model shocks correctly. Finally, the transport subroutine is written in sliding-rezone form, which means that the mesh at the beginning and the end of the timestep need not be the same. Since the algorithm is one-dimensional, timestep splitting is employed to solve the 2-D problem.

The fluid transport routine JPBFACT is fully vectorized and requires about 2 μ s per meshpoint-cycle. This time would have been still less if a vectorized fully two-dimensional routine had been used, since the 1-D loops are too short to permit full advantage to be taken of the vector capabilities of the NRL ASC. The table lookup in the EOS was also fully vectorized, so that pressure calculations required about 20% of the time needed for the hydrodynamics. These two items took up nearly all of the running time in the blast calculation itself. The cost of initialization was negligible, but the diagnostics cost up to 30% as much as the hydrodynamics, depending on how many of the various possible quantities were actually plotted. This latter number would be greatly reduced if the plot routines were fully vectorized.

A version of the AFWL 1 KT standard (Ref 8) was used to initialize the energy, density and velocity (flow field) at 3.76 milliseconds. The corresponding shock radius was 103.9 ft (31.69 m) peak overpressure of 1645 psi (1.134×10^4 K Pa). Because some areas of the grid were very coarse, interpolation onto the grid was performed. After the 1 KT flow was laid down inside a radius of 104 feet (31.7 m) the fine-zoned grid was activated to follow the peak pressure as it moved along

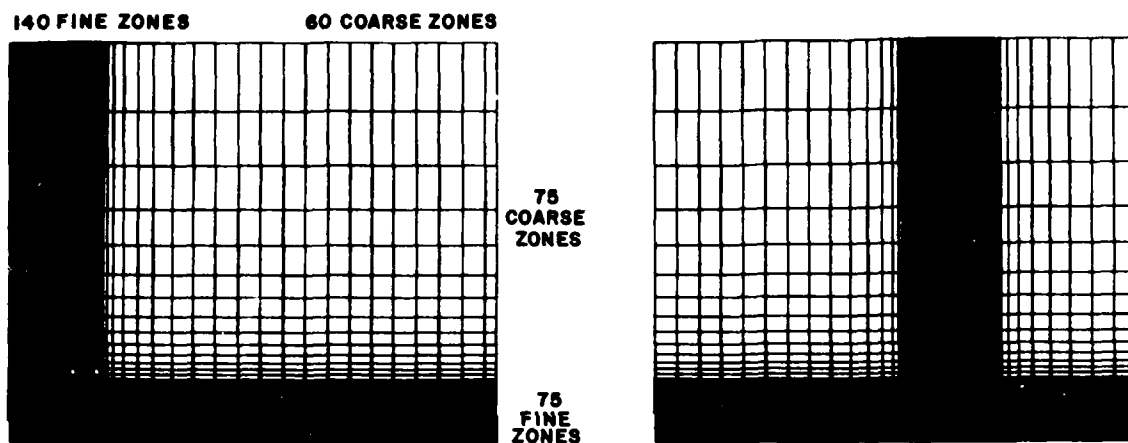


Fig. 3 - Adaptive gridding. The grid at initialization and at transition point (lines are drawn for every other zone, lines in fine-zone region are indistinguishable).

the ground surface, modelled as a perfectly reflecting boundary. This region comprised 140 zones, and a switch was set to keep 40 of these zones ahead of the reflection point. Permeable boundary conditions were used on the top and right edges of the mesh; i.e., density, pressure and velocity were set equal to ambient preshock conditions. Reflecting conditions were applied to the left and bottom.

The timestep was recalculated at every cycle according to the Courant condition

$$\Delta t = 0.5 \min_{i,j} \frac{(\Delta x_i, \Delta y_j)}{(c + |V|)_{ij}}, \quad (1)$$

where c is the speed of sound and $|V|$ is the modulus of the flow speed. This could have been relaxed somewhat by allowing violation of the local Courant limit at points ("hot spots") far from the region of chief physical interest. The total elapsed time in the 2-D calculation, 7.6 ms, required 5600 cycles.

Three types of diagnostics were employed, all in the form of plots made by post processing a dump tape. The first type of diagnostic consisted of CRT contour plots of density and static pressure, and arrows indicating the magnitude and direction of the velocity field, obtained at the dump intervals (every 200 cycles). The second type was pressure-range curves at $z=0$, obtained by finding the pressure peak(s) along the ground at each dump interval and hand-plotting them on the same graph. The third type consisted of pressure histories at a series of 24 stations, obtained by saving the energy and mass densities and the velocities at every cycle.

IV. RESULTS AND PHENOMENOLOGY

This calculation has been done to understand the violent effects of 1 KT of energy being released in the atmosphere at a HOB of 104 ft (31.7m). A strong spherical shock is created in the surrounding air, and reflects from the ground.

The outward-traveling airblast is then composed of two parts: one reflected upward approximately normal to the ground, and the original spherical blast. The peak pressure is coincident with the intersection of the two waves. This intersection continues to move outward until the angle of the spherical shock with respect to the ground reaches a critical value and the transition to a double Mach stem occurs. As shown by Ben-Dor and Glass (Ref. 9), this angle depends upon the incident strength of the shock (Fig. 4). Shocks with Mach numbers greater than 10 are not shown. Initially, the Mach number for the HOB simulation is well above 10. The Mach number at transition is approximately 11 and the angle is less than 50° . From Fig. 4 the corresponding region is double Mach reflection.

Figure 1 has been labeled with the notation of Ben-Dor and Glass (Ref. 9). It should be noted that what is generally regarded as the second Mach stem is in fact the second reflected wave, which is part of the second Mach structure. To be consistent, one must label the second Mach stem as M_1 at the indicated location. The definition used is the state of the fluid one obtains by passing through one shock wave (M_1) or two shock waves (R and R_1). The first reflected wave R becomes the incident wave for the second Mach structure. Density contours are shown in Fig. 5 for an planar shock on wedge with a Mach number of 7 and an angle of 50° . The complimentary figure illustrates the proper labeling of the multiple waves. Comparison of Fig. 5 and the HOB simulation (Fig. 6) shows that corresponding waves can be identified. Differences between the planar shock on wedge and the HOB can be explained in terms of the unsteady nature of the HOB case (a spherically expanding wave that continuously decreases in Mach number and angle.) Although the term irregular Mach reflection has been used to describe the complex shock structure that evolves from HOB events, we believe it to be very regular and explainable as a double Mach reflection that evolves as a function of time.

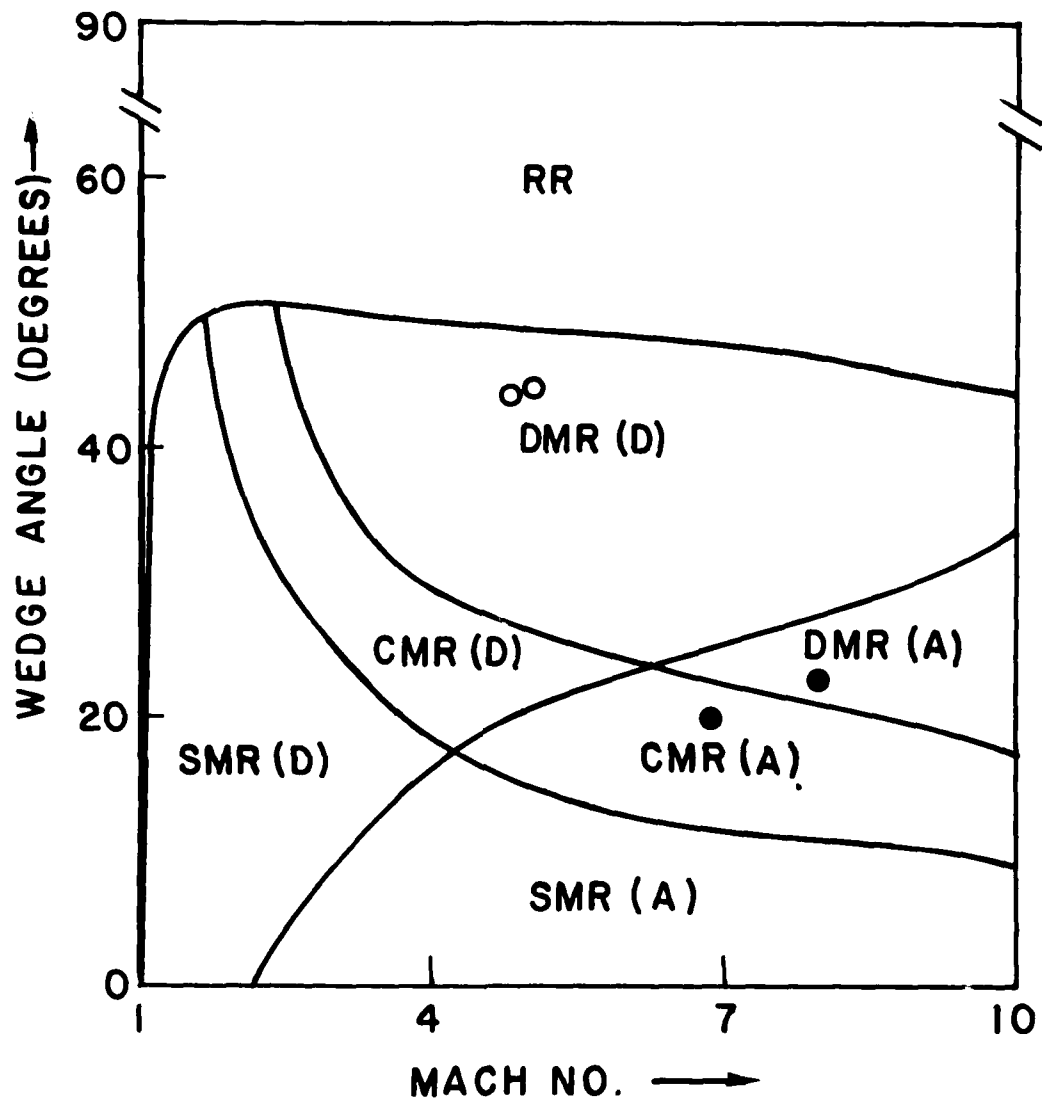


Fig. 4 - Types of shock reflection: RR, CMR, SMR, and DMR denote regular reflection and single, complex and double mach reflection, respectively. The D and A refer to attached and detached shocks.

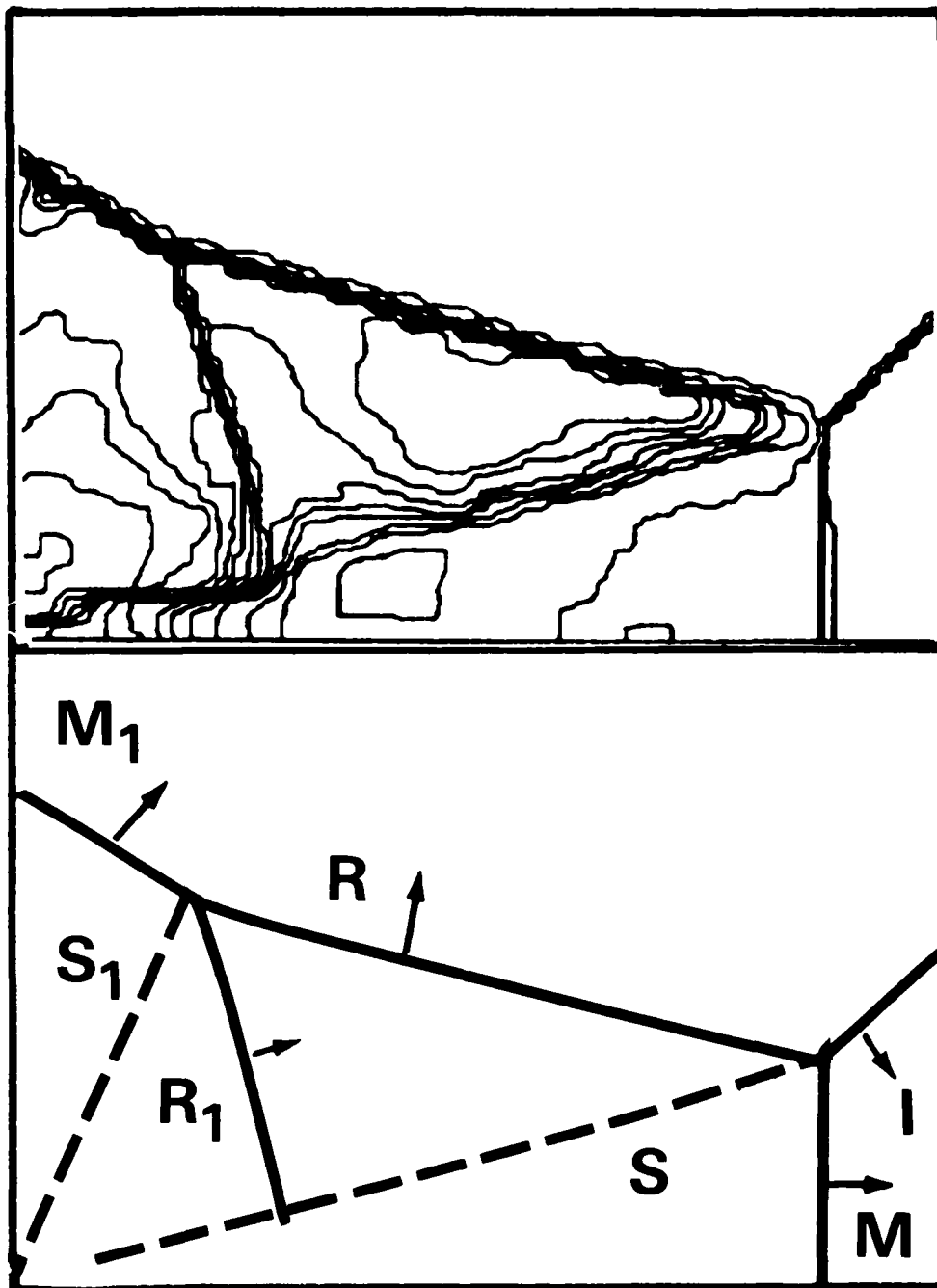


Fig. 5 - Planar shock (Mach 7) on 50° wedge with wave identification

The HOB numerical simulation begins just before the shock first reflects from the ground. As a summary of how the flow field then develops, we present snap-shots at the important stages. (A more complete display is presented in Appendix A). Figure 6a indicates the pressure and density contours and velocity vectors at $t = 3.18$ ms. In Fig. 6b the reflected shock is shown moving upward, the outward flow begins to stagnate at the ground (transition). Fig. 6c, at $t = 5.99$ ms, shows an enlargement of the shock front, and the development of the Mach stem, slip surface and second Mach stem. The angle of the shock with respect to the ground is increasing with time, so that the effective wedge angle is decreasing. From the work of Ben-Dor and Glass one expects a transition to double Mach stem to occur at approximately 45° . The angle in Fig. 6b is about 45° and the shock front has entered the transition phase. Figure 6d shows the fully developed shock structure at 7.79 ms. Toeing out of the first Mach stem can be also seen in the contours of Fig. 6d and occurs as the fluid rolls forward where the slip line would otherwise intersect the ground. The velocity field in Fig. 6d also shows this detail.

Note the reflected shock properties (that part of the structure that contains the second Mach stem M_1). The reflected shock propagates rapidly through the high temperature fireball, due to the high local sound speed. The shape of this reflected wave is a primary difference between the HOB case and the planar wave on wedge case. The other major difference, of course, is the spherically expanding blast wave which decreases in strength approximately as r^{-2} .

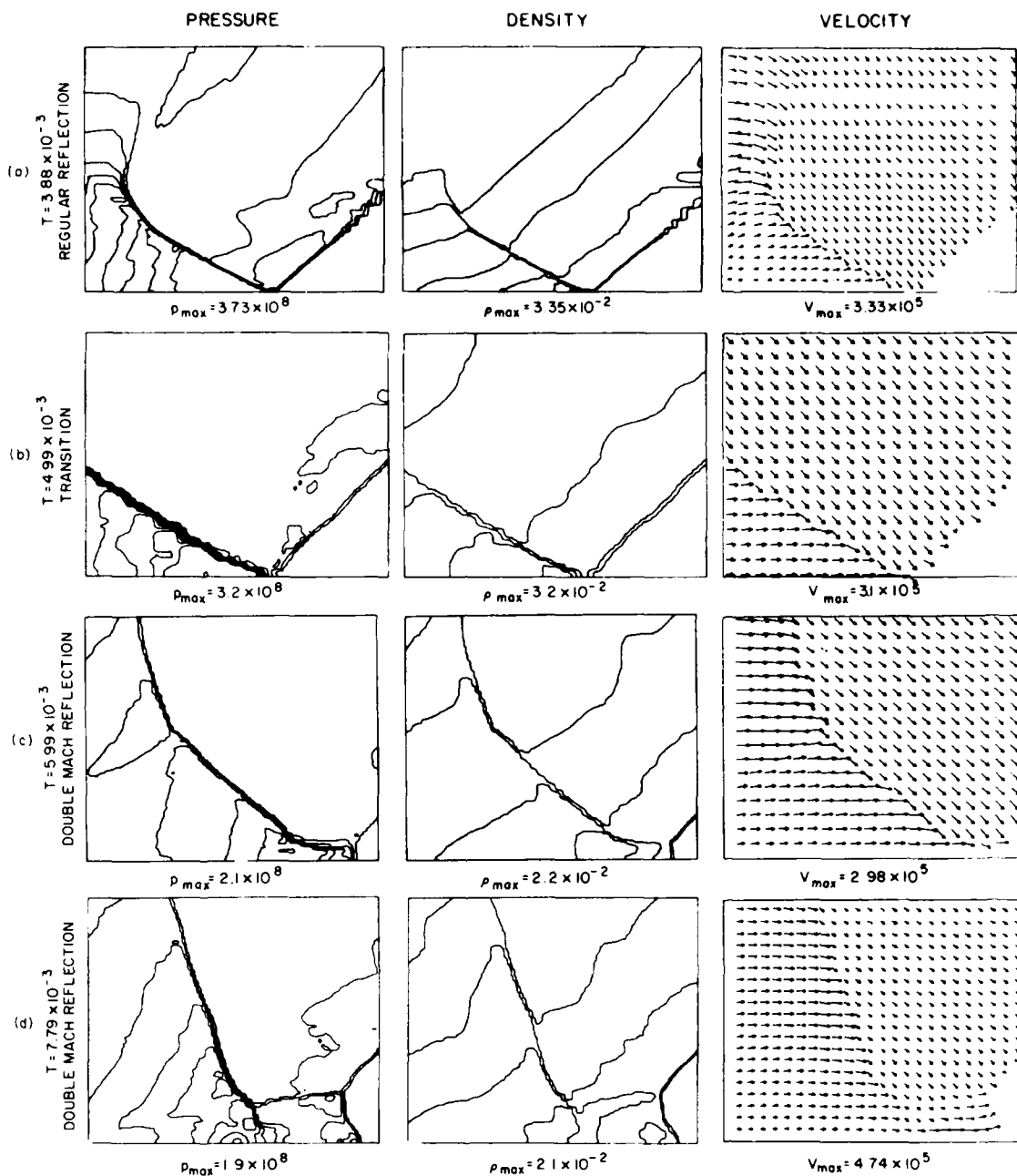


Fig. 6 - Pressure, density, and velocity fields for HOB calculation (a) in regular reflection state; (b) at transition to Mach reflection; (c) shortly afterward, when second peak has become larger than first; and (d) fully developed (note toe at base of first Mach stem). Units in cgs.

An effective way to quantitatively evaluate the calculation and observe in detail the transition to a Mach stem regime can be seen by examining the station data. The station sensors were placed in the bottom row of the calculation 100 to 200 cm apart. In Table I the maximum pressure recorded for each station along with the location can be found.

Besides giving a reliable value for the peak pressure to be used for constructing the pressure-distance curve, these data allow one to see effects fixed in space but varying in time. Figure 7 is a superposition of the pressure profiles from stations 15 to 24 (the transition region). Noteworthy is the profile from station 17, which is the first station to record a second peak on the back side. At station 19, 200 cm further away from ground zero, the second peak is almost equal to the first. The visible transition (as seen in Fig. 6b, occurs at a ground range between 3100 cm and 3300 cm (stations 19-21) revealing a dominant second peak and a "first peak" (i.e., first seen by the sensor) that is about half the magnitude of the second. The second peak does not exhibit a sharp almost discontinuous rise and then a rapid but slower decrease along the back side. Instead, it has the appearance of a density compression. This behavior has dramatic consequences for military planners because the pressure-distance curve is modified and the dynamic pressure is enhanced.

The analogous profiles for dynamic pressure are presented in Fig. 8. Again data from stations 15 to 24 is utilized. The development of the second peak and its correlation with the Mach stem formation can be observed. There is, in addition, a noticeable increase in the first peak values (station 15 to the maximum at station 18). After the structure becomes visibly resolved (station 20 and beyond) the second peak resembles a rounded profile suggesting the formation of a stagnation region behind the first peak (Mach stem).

Table 1

Station No.	Location (cm)	Time (sec)	Pres (dynes/cm ²)
1	2.0000E 02	2.25E-04	8.11E 08
2	4.0000E 02	2.80E-04	7.92E 08
3	8.0000E 02	5.28E-04	7.17E 08
4	1.0000E 03	7.23E-04	6.73E 08
5	1.2000E 03	9.54E-04	6.24E 08
6	1.4000E 03	1.23E-03	5.65E 08
7	1.6000E 03	1.54E-03	5.21E 08
8	1.8000E 03	1.91E-03	4.70E 08
9	2.0000E 03	2.34E-03	4.54E 08
10	2.2000E 03	2.81E-03	4.14E 08
11	2.3000E 03	3.07E-03	4.03E 08
12	2.4000E 03	3.35E-03	3.92E 08
13	2.5000E 03	3.62E-03	3.82E 08
14	2.6000E 03	3.88E-03	3.73E 08
15	2.7000E 03	4.19E-03	3.37E 08
16	2.8000E 03	4.48E-03	3.33E 08
17	2.9000E 03	4.79E-03	3.05E 08
18	3.0000E 03	5.11E-03	3.01E 08
19	3.1000E 03	5.41E-03	2.33E 08
20	3.2000E 03	6.06E-03	1.96E 08
21	3.3000E 03	6.49E-03	1.79E 08
22	3.4000E 03	6.82E-03	1.87E 08
23	3.5000E 03	7.28E-03	1.85E 08
24	3.6000E 03	7.73E-03	1.69E 08

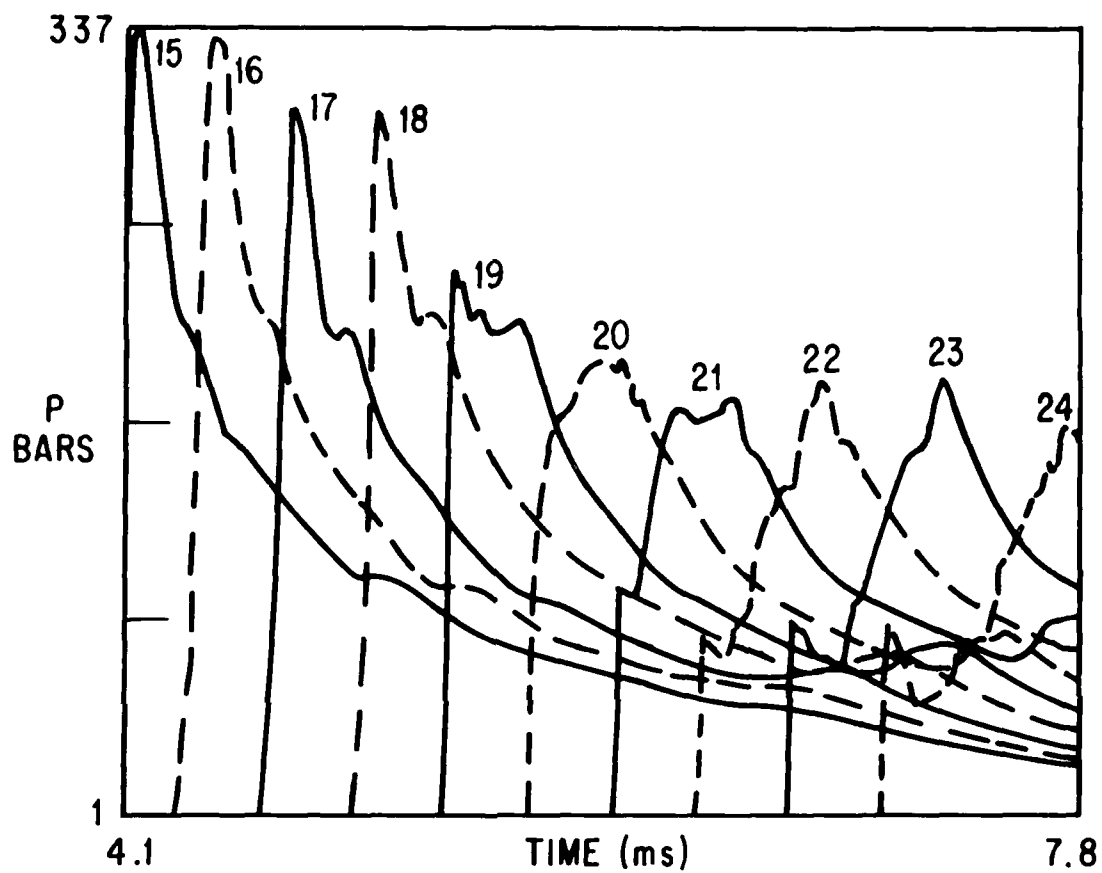


Fig. 7 - Station pressure data (nos. 15-24)

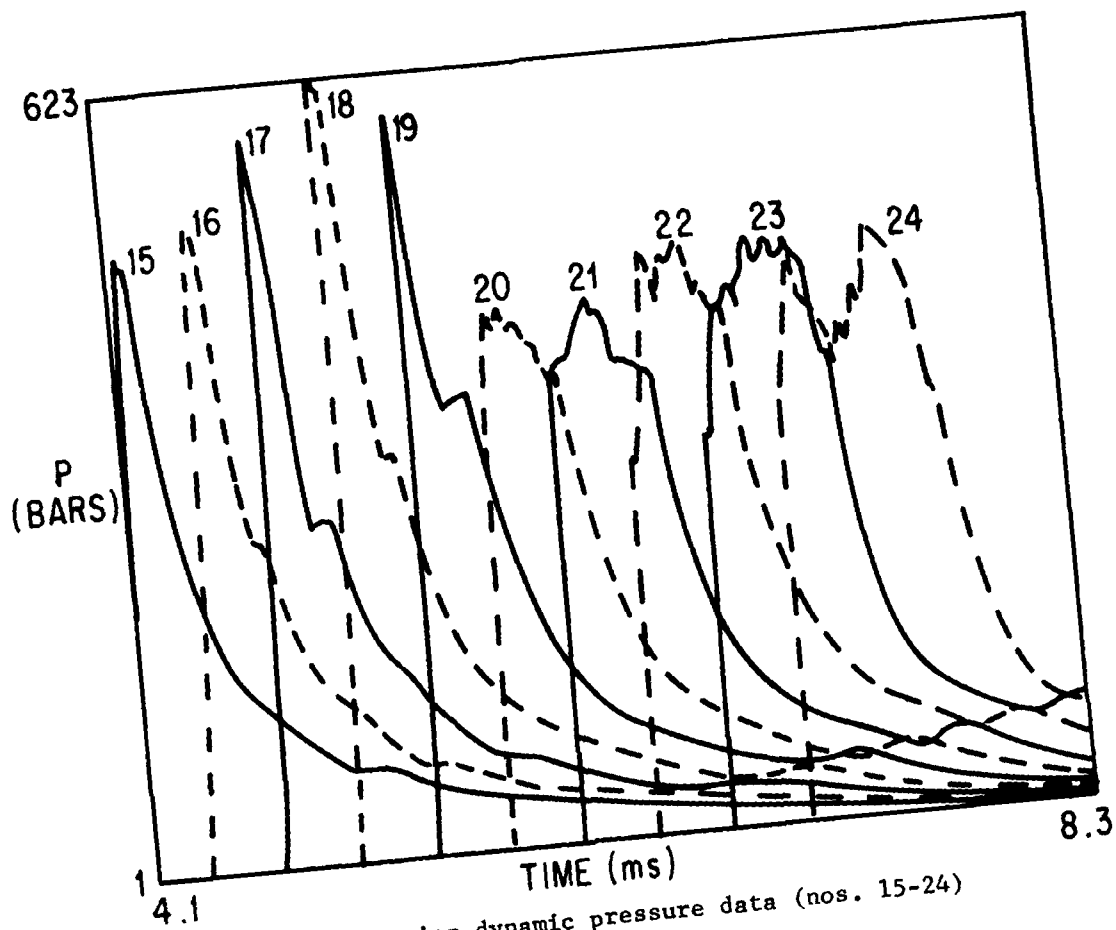


Fig. 8 - Station dynamic pressure data (nos. 15-24)

Finally we consider the pressure-distance relation for the HOB case. In Fig. 9 we compare the results of the numerical simulation with the data of Carpenter and with empirical analysis. Carpenter's data are based upon careful HOB experiments with 8 lb PBX9404 spheres. The empirical analysis was based on a 1 KT nuclear free air curve and HOB construction factors. The calculated values in the regular reflection regime are 20% low, which may be attributed to a combination of FCT clipping, the resolution of the grid, and inaccuracies in the initialization of the flow field. During and after Mach reflection, the peaks remain low until the Mach stem structure has grown large enough to be resolved on the mesh. By the time it occupies a region of 15 cells high and 35 cells wide, the peak pressures are in good agreement with the HE data and the empirical analysis.

Other attempts to model the transition region have been made. Needham and Booen (Ref. 10) present results of a 1100 lb pentolite sphere at 15 feet HOB. The general phenomena of the flow field can be seen from their simulation. When a pressure distance curve is constructed from this calculation, one finds that in the regular reflection region their results are 15% to 30% high relative to theory. After transition to double Mach reflection the first peaks are 20% low while the second peaks are 40% low (Ref. 4).

V. SUMMARY

The airblast from a 1KT nuclear event at 104 ft HOB has been numerically simulated with the FAST2D computer code. The results give insight to the formation and subsequent evolution of the Mach stem, the triple point, and the contact discontinuity. The transition from regular reflection to double Mach reflection is predicted. We suggest that the first signal for

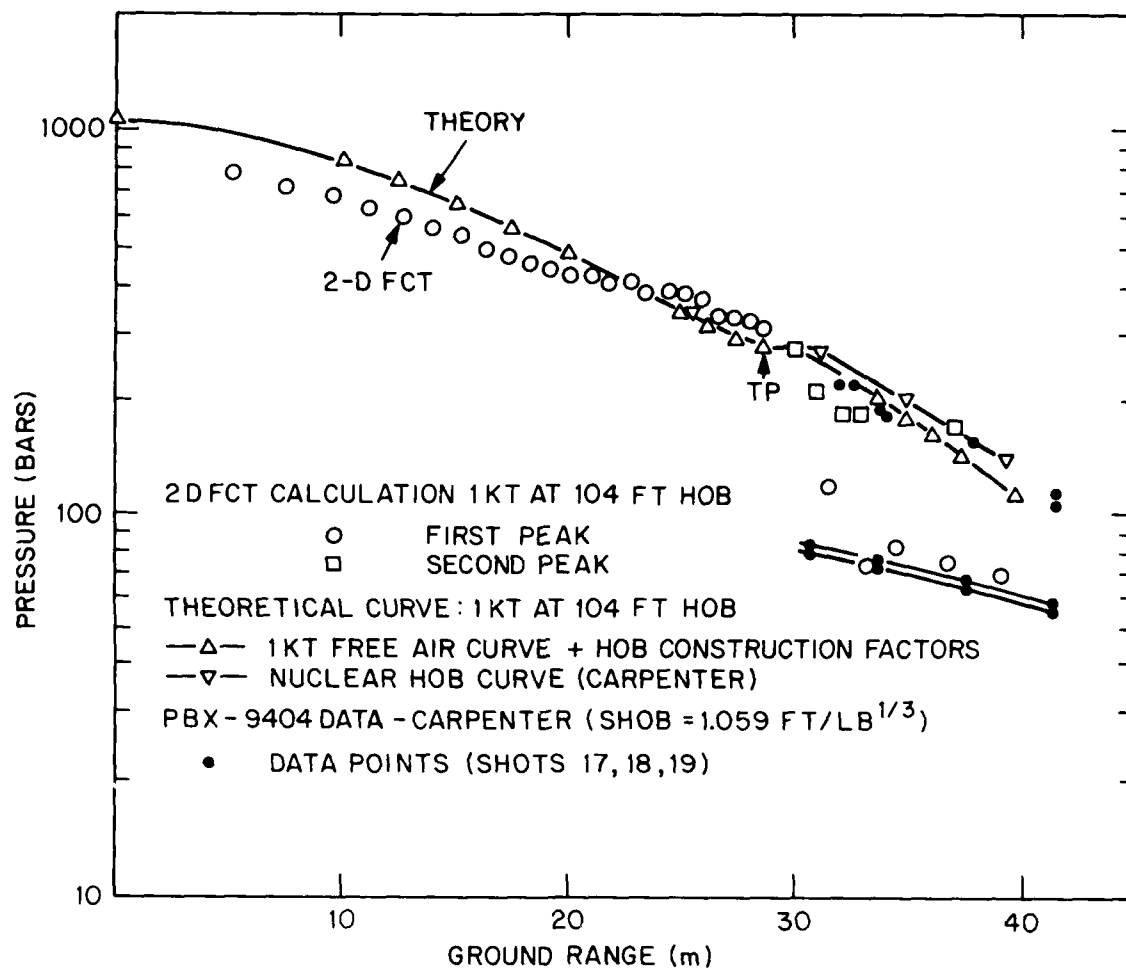


Fig. 9 - Pressure-range curves for first and second (after transition - denoted by TP - to double Mach reflection) peaks

transition is the appearance of a second peak behind the shock front due to stagnation in the flow. Comparison with the pressure-distance curves of Carpenter and Kuhl indicates agreement within 20%. Both first and second peaks are predicted with similar accuracy.

ACKNOWLEDGEMENT

We are grateful to Dr. Allen Kuhl of R&D Associates for his valuable advice and technical guidance.

This work was supported by the Defense Nuclear Agency under Subtask Y99QAXSG, work unit 00001, work unit title, "Flux-Corrected Transport."

References

1. Boris, J.P., Flux-Convected Transport Algorithms for Solving Generalized Continuity Equations, NRL Report #3237 (1976)
2. Boris, J.P., Book, D., "Flux-Corrected Transport I: SHASTA, a Fluid Transport Algorithm that Works", J. Comp. Phys., 11, 38 (1973).
3. Carpenter, H.J., Height-of-Burst Blast at High Overpressure, 4th International Symposium on Military Applications of Blast Simulation (1974).
4. Kuhl, A. (Private Communication, 1981).
5. Gilmore, F.R., "Equilibrium Composition and Thermodynamic Properties of Air to 24,000°K", RM-1543 (Aug 1955).
6. Young, T.R. (Private Communication, 1981).
7. Book, D., Boris, J., Kuhl, A., Oran, E., Picone, M., and Zalesak, S. Simulation of Complex Shock Reflections from Wedges in Inert and Reactive Gaseous Mixtures, Proceedings of Seventh International Conference on Numerical Methods in Fluid Dynamics, Springer-Verlag, Stanford, 1980.
8. Needham, et al., AFWL 1 KT Nuclear Airblast Standard, AFWL TR-73-55, Air Force Weapons Laboratory (April 1975).
9. Ben-Dor., Glass I.I., Domains and Boundaries on Non-Stationary Oblique Shock-Wave Reflections, I. Diatomic Gas, J. Fluid Mechanics, Vol. 92, Pt. 3, pp. 459-496 (1979).
10. Booen, M.W., and Needham, C.E., Two Dimensional Hull Code Simulation of Complex and Double Mach Reflections, Technical Note No. NTE-TN-81-001, Air Force Weapons Laboratory, New Mexico, January 1981.

APPENDIX A. DETAILED TIME HISTORY OF CALCULATION

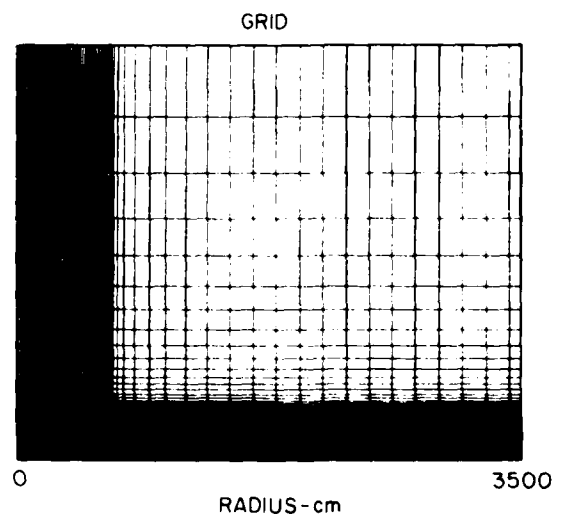
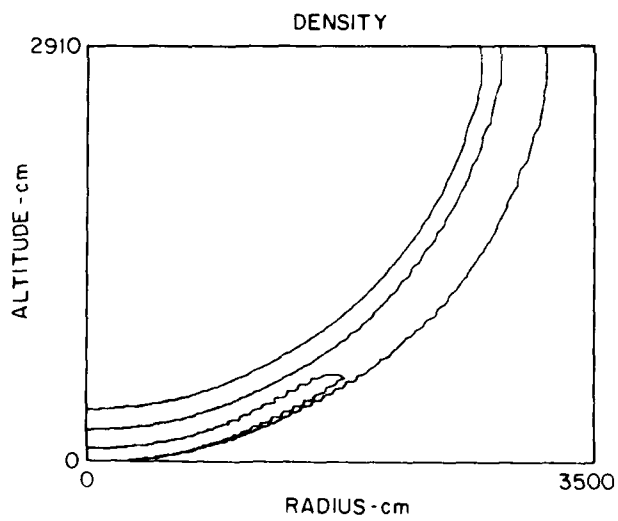
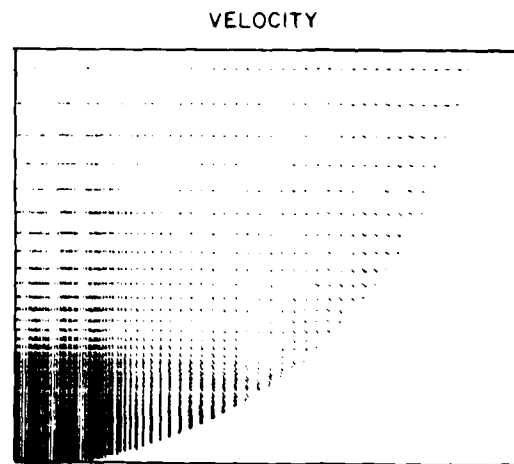
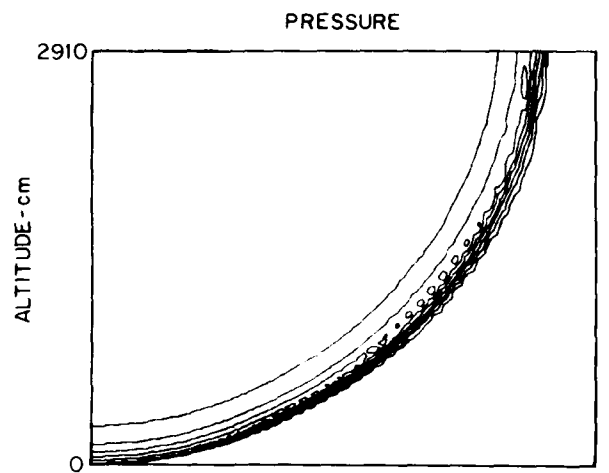
The following figures comprise a temporal history of the numerical simulation. Each page contains pressure contours, velocity vectors, density contours, and the corresponding grid for a particular time.

The series begins at $t_o = 0$ ($t_I = 3.76$ ms) and continues to $t_F = 8.28$ ms.

1 kt AT 104 ft HOB

TIME = 0.0 msec

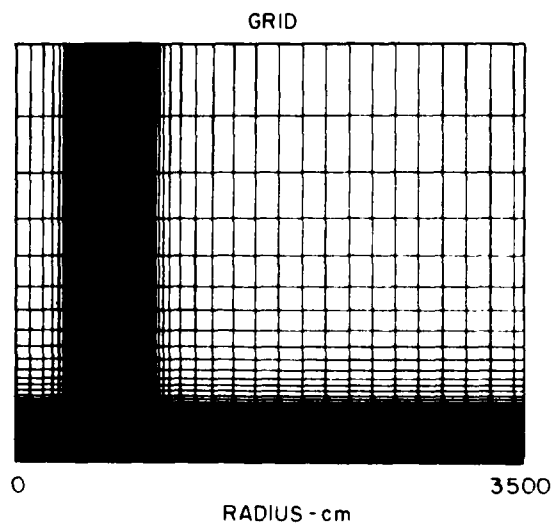
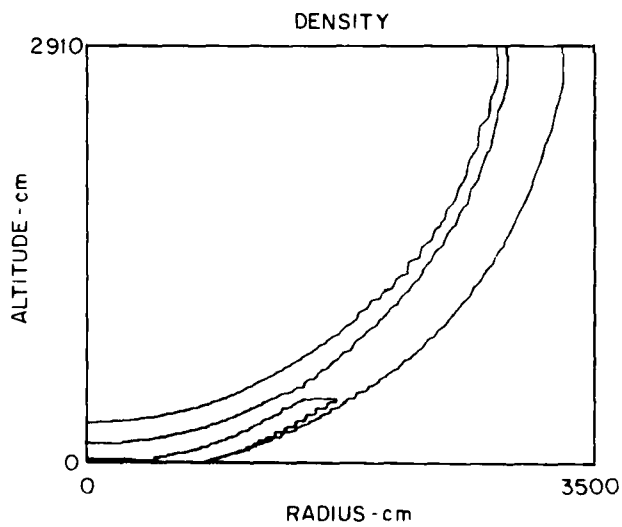
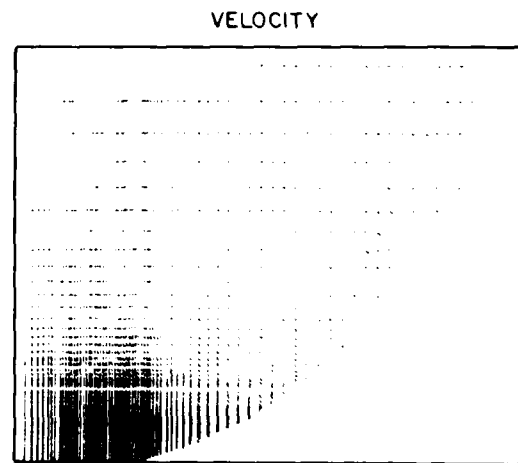
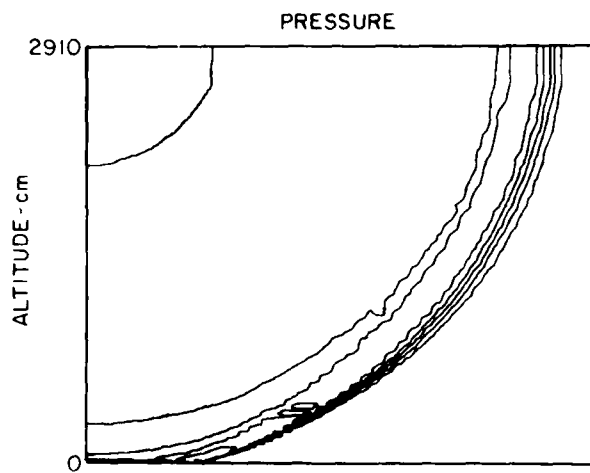
CYCLE = 0



1 kt AT 104 ft HOB

TIME = 0.34 msec

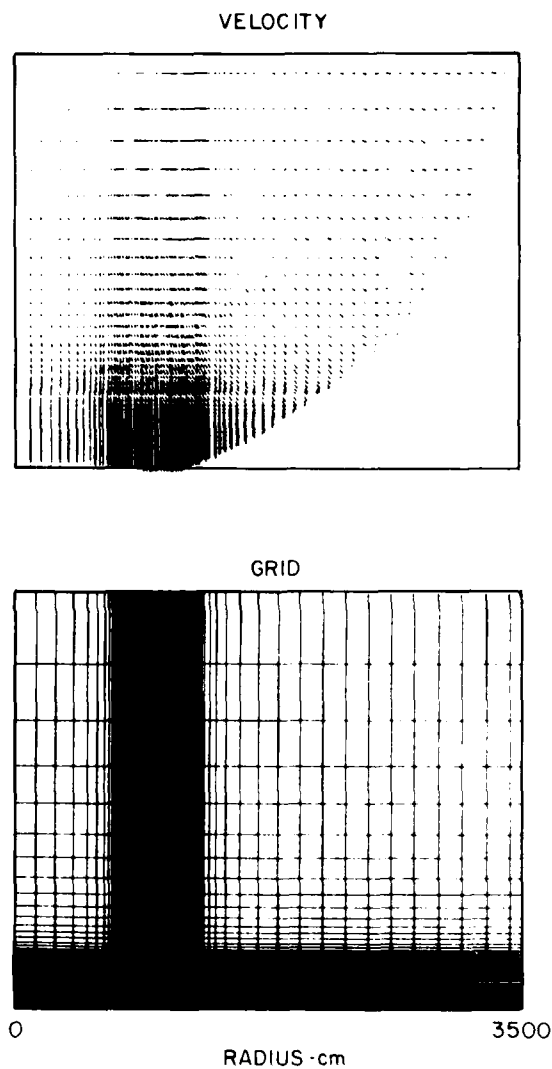
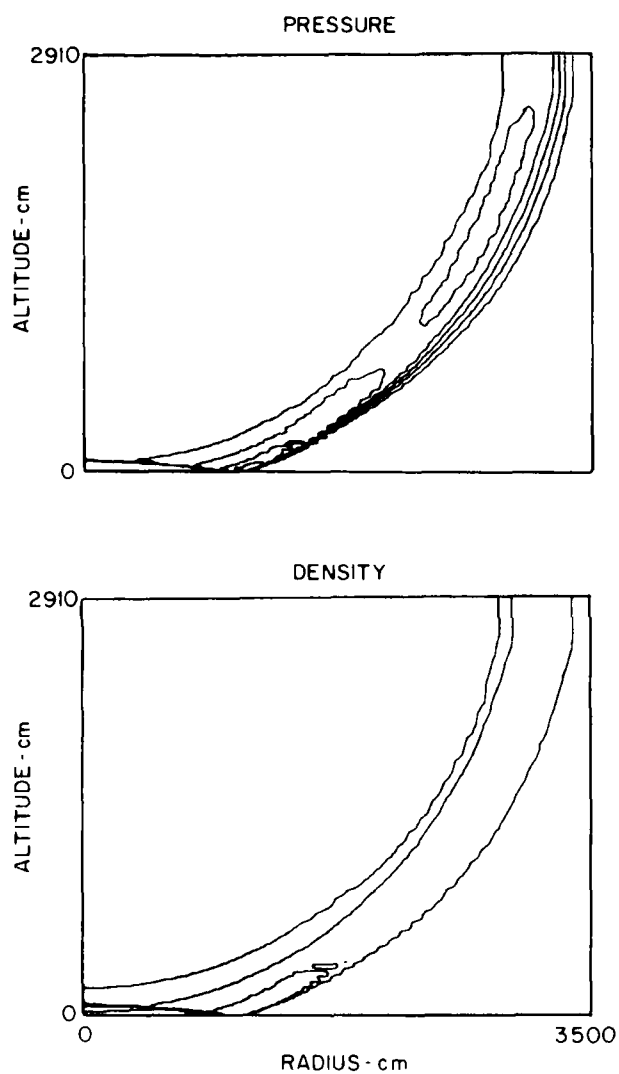
CYCLE = 400



1 kt AT 104 ft HOB

TIME = 0.91 msec

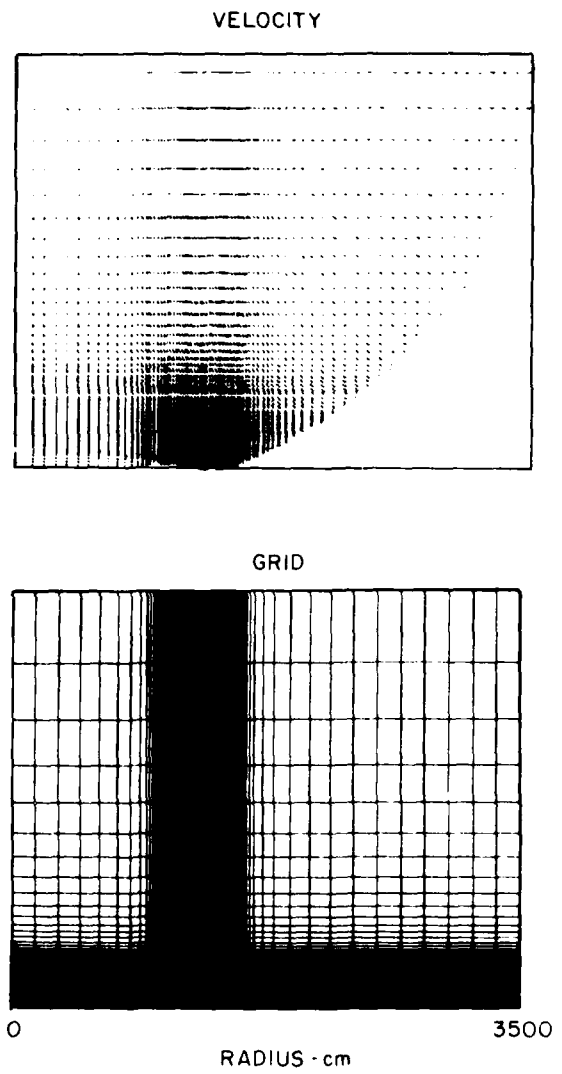
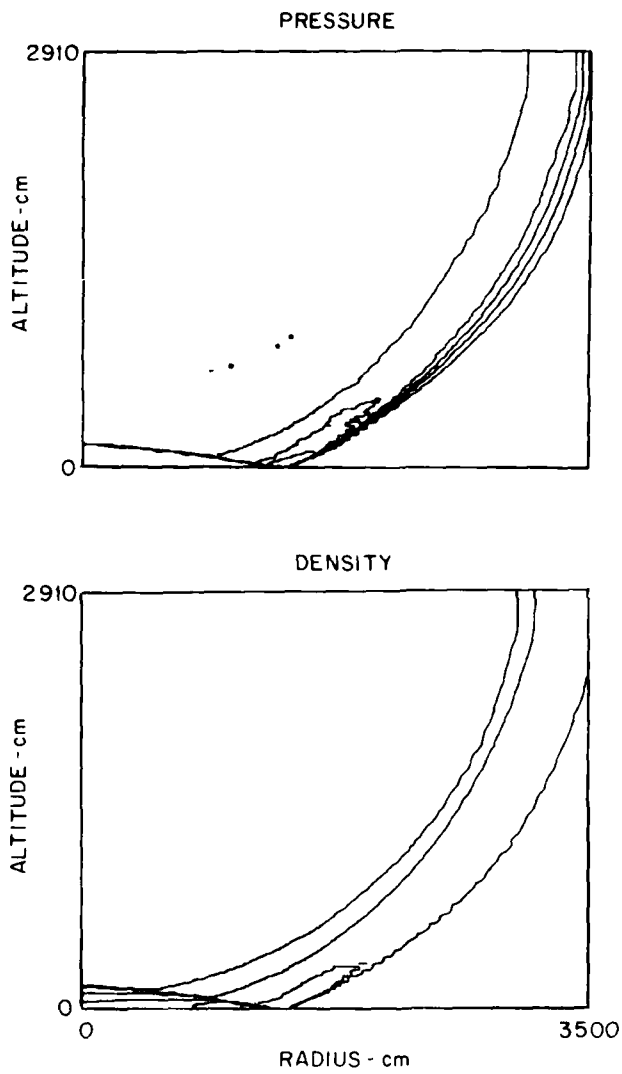
CYCLE = 800



1 kt AT 104 ft HOB

TIME = 1.05 msec

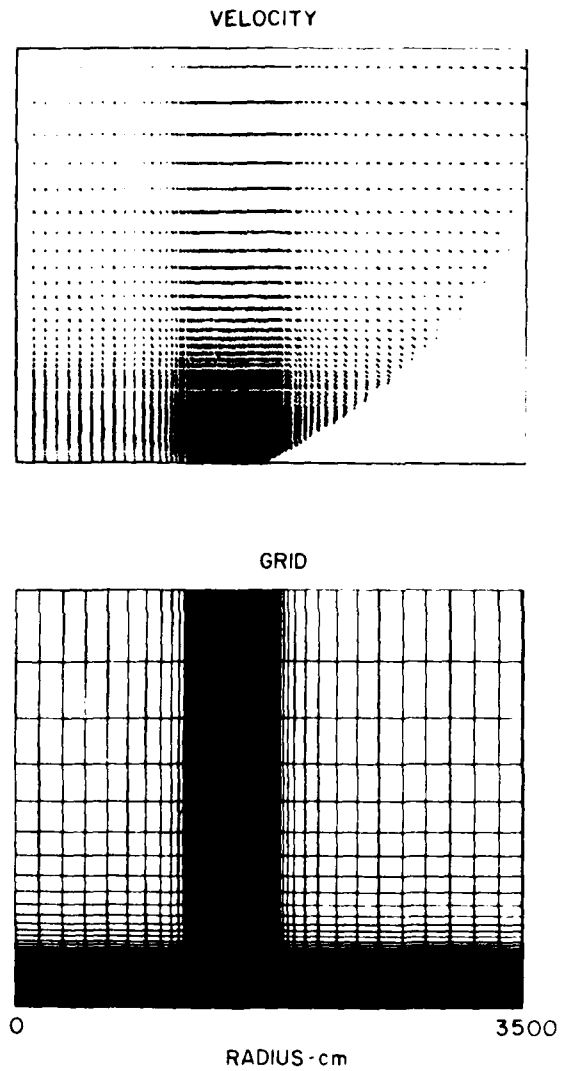
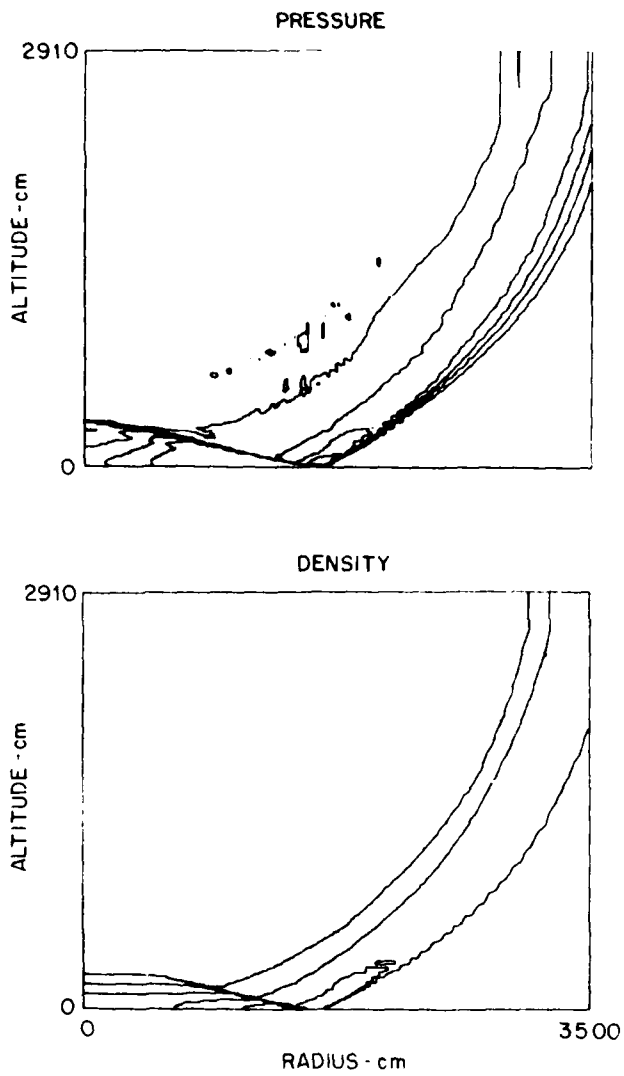
CYCLE = 1200



1 kt AT 104 ft HOB

TIME = 1.42 msec

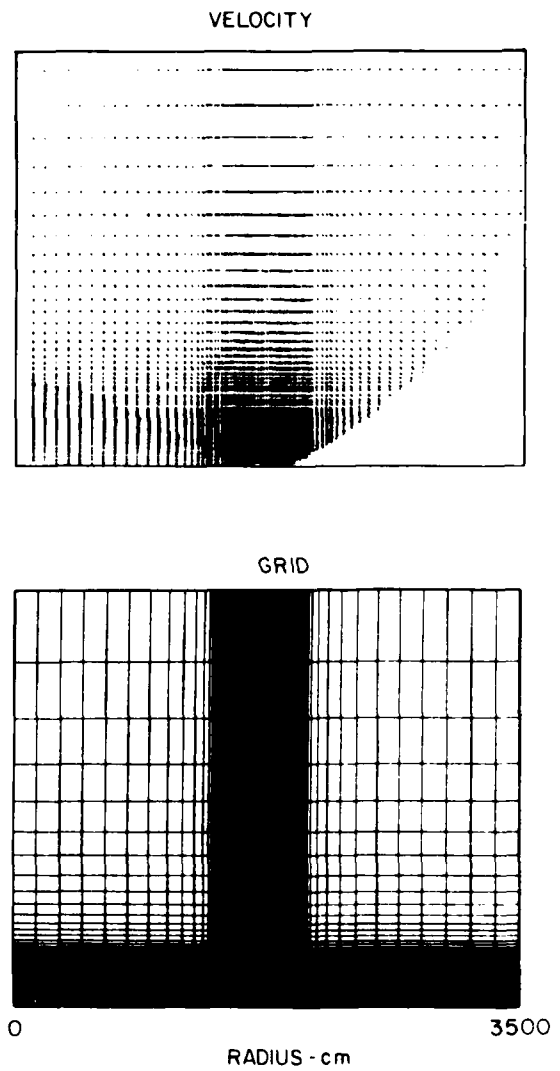
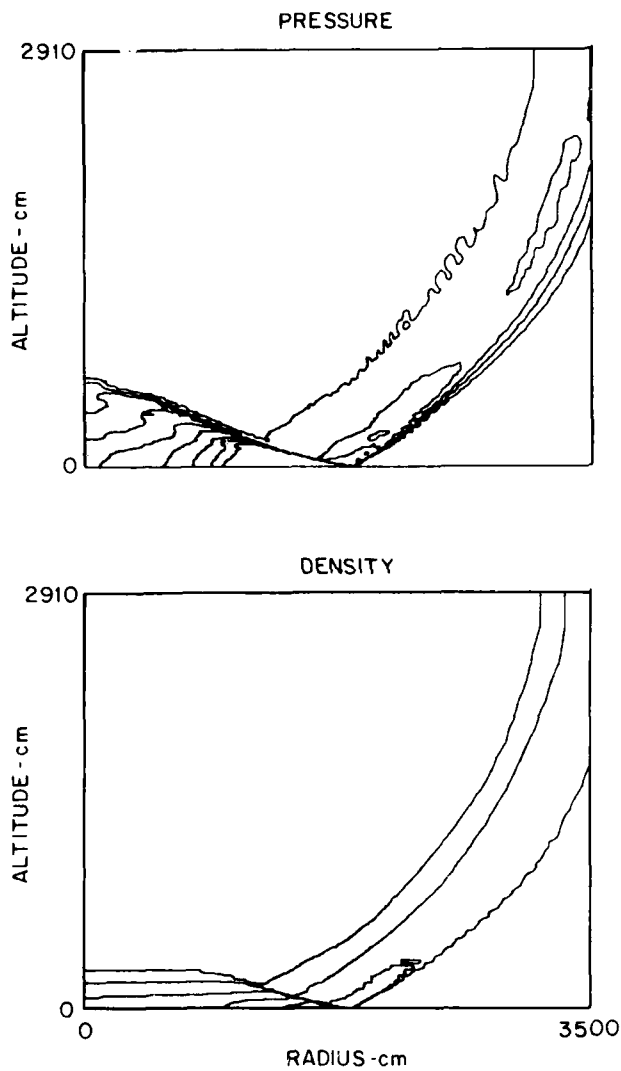
CYCLE = 1600



1 kt AT 104 ft HOB

TIME = 1.80 msec

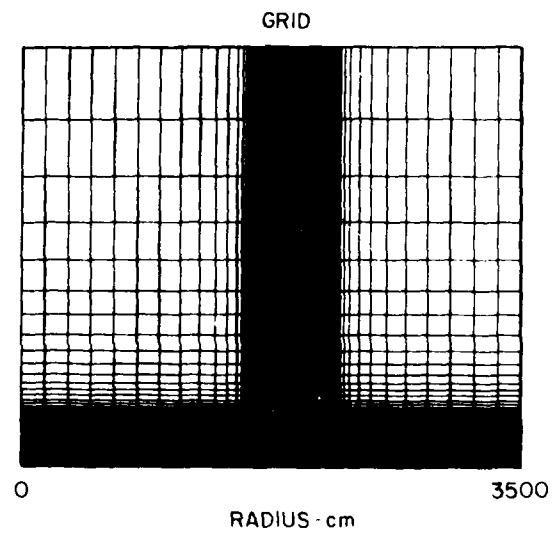
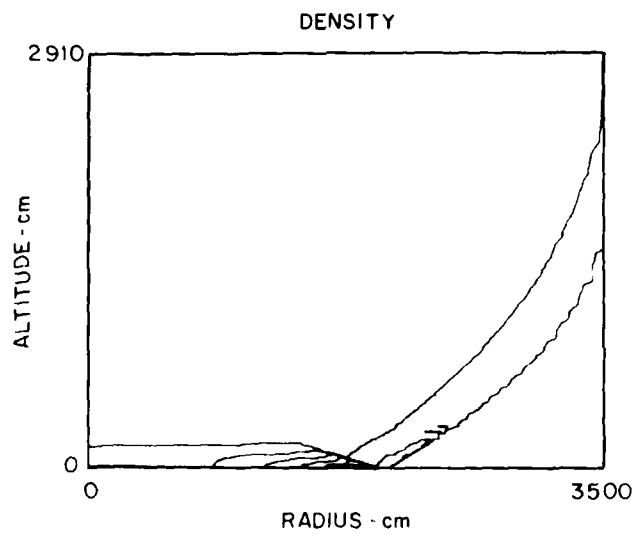
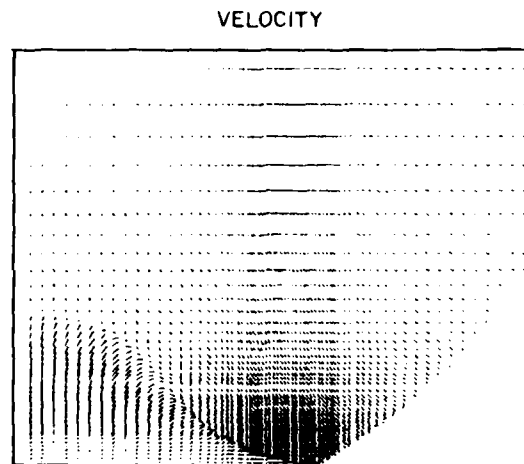
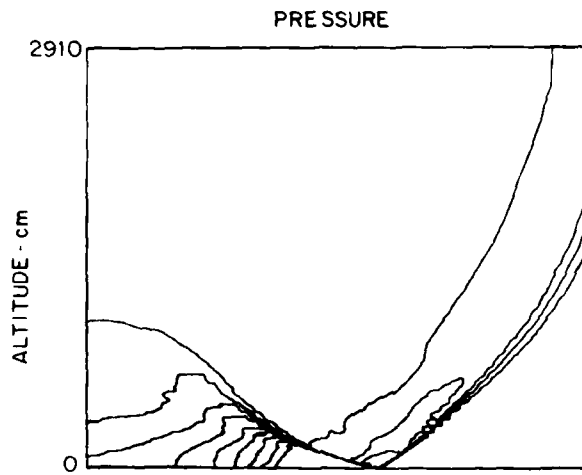
CYCLE = 2000



1 kt AT 104 ft HOB

TIME = 2.20 msec

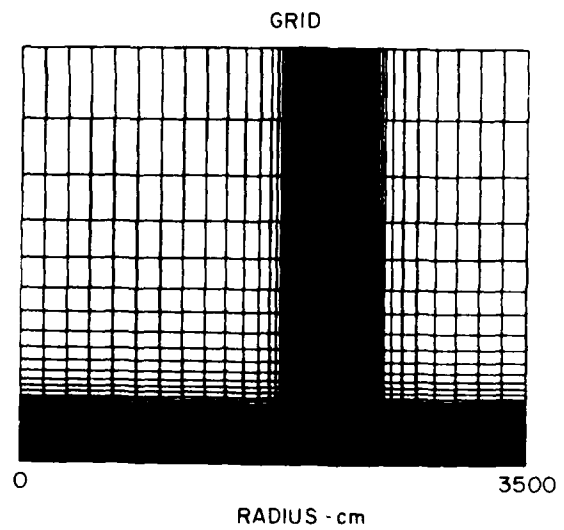
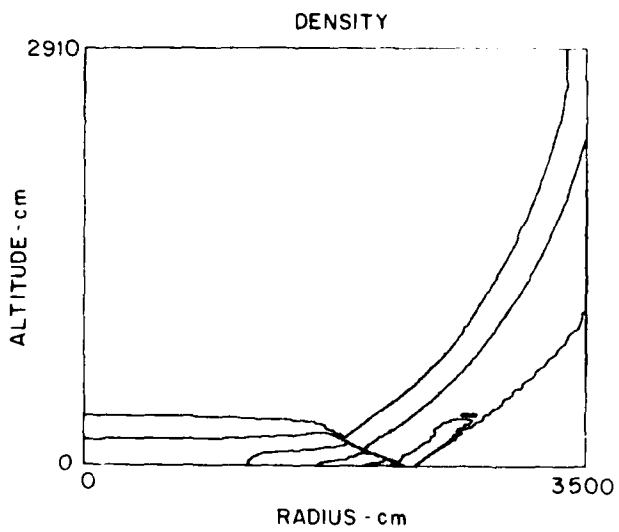
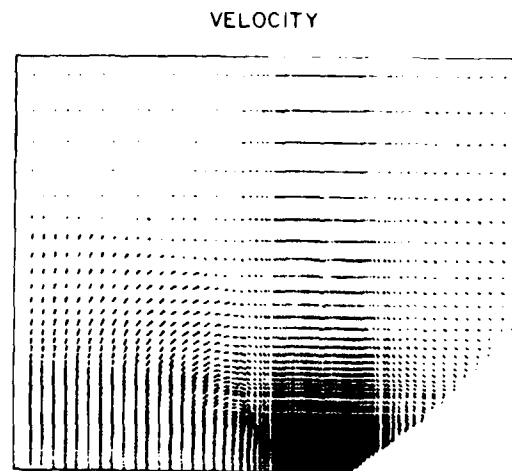
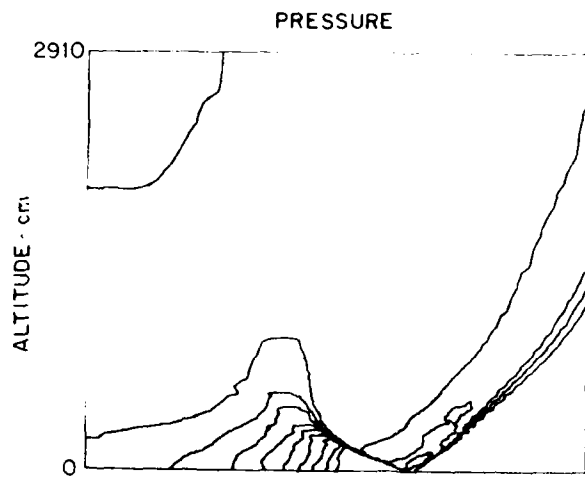
CYCLE = 2400



1 kt AT 104 ft HOB

TIME = 2.81 msec

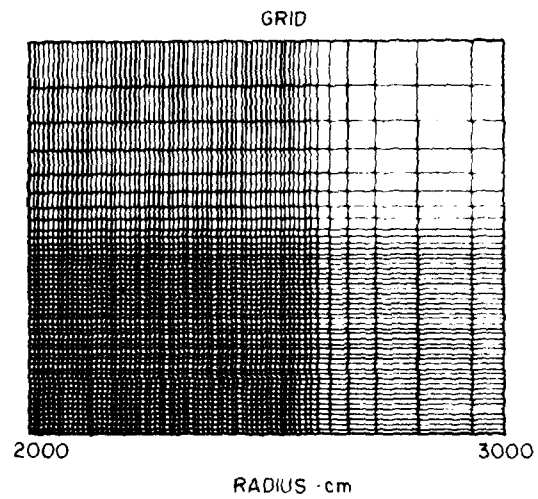
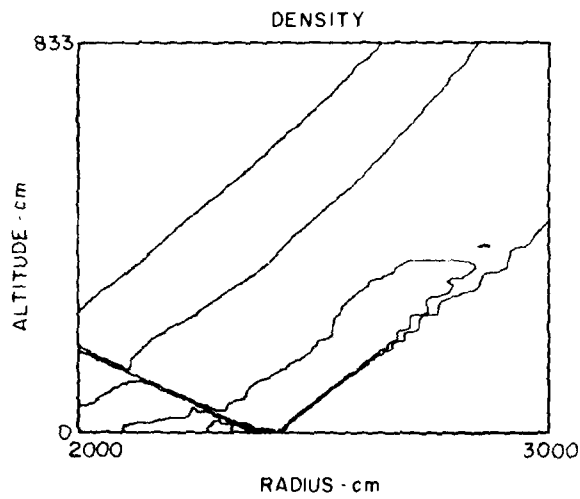
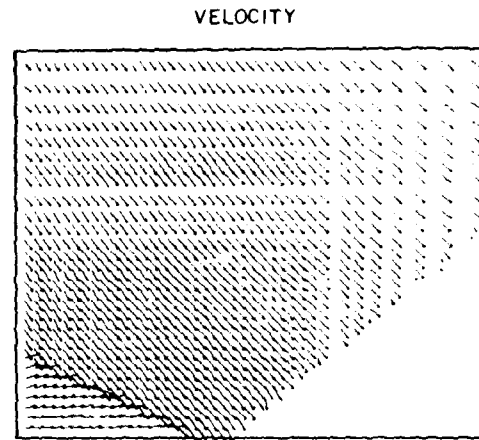
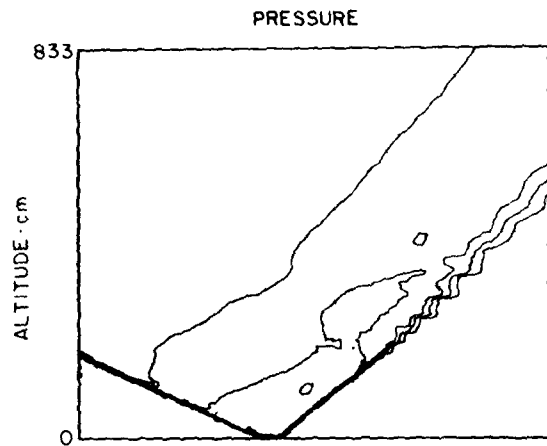
CYCLE = 3000



1 kt AT 104 ft HOB

TIME = 3.24 msec

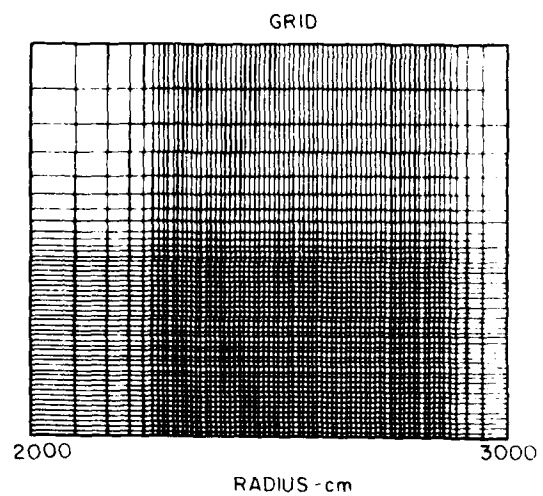
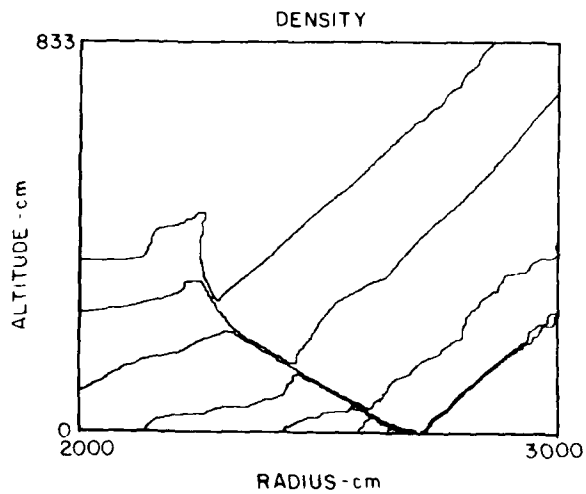
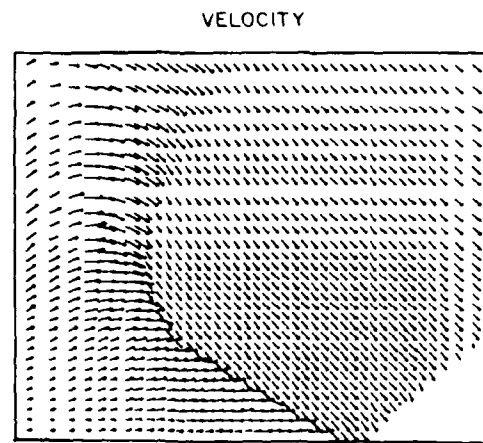
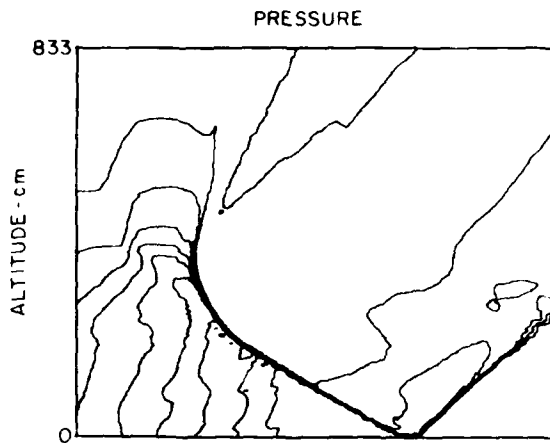
CYCLE = 3400



1kt AT 104 ft HOB

TIME = 4.10 msec

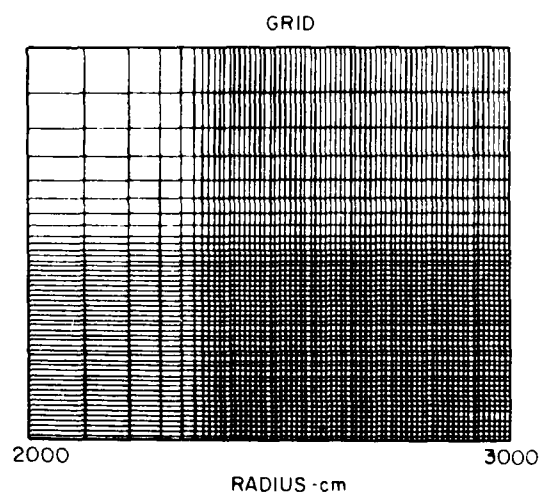
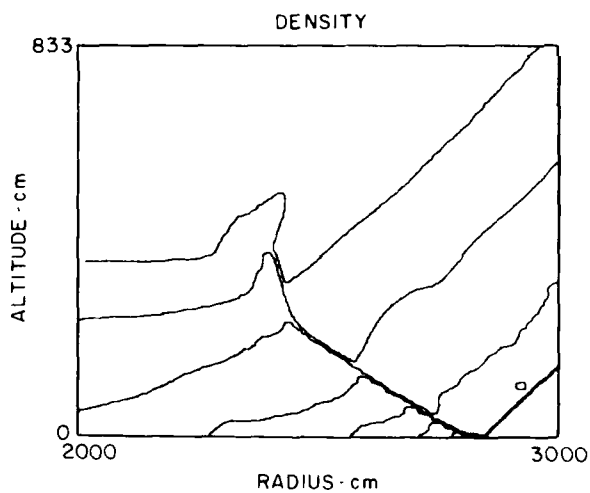
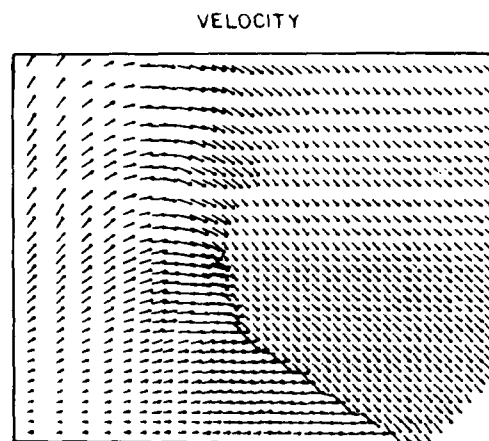
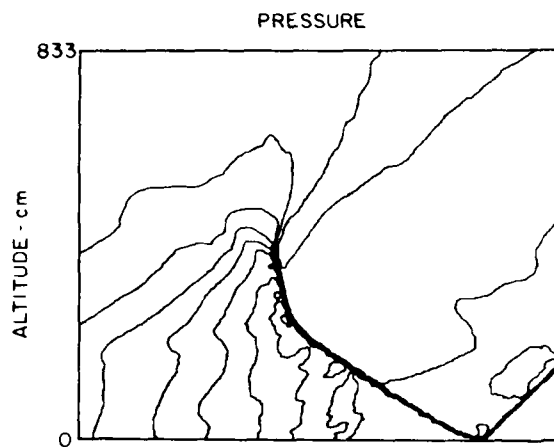
CYCLE = 4200



1 kt AT 104 ft HOB

TIME = 4.54 msec

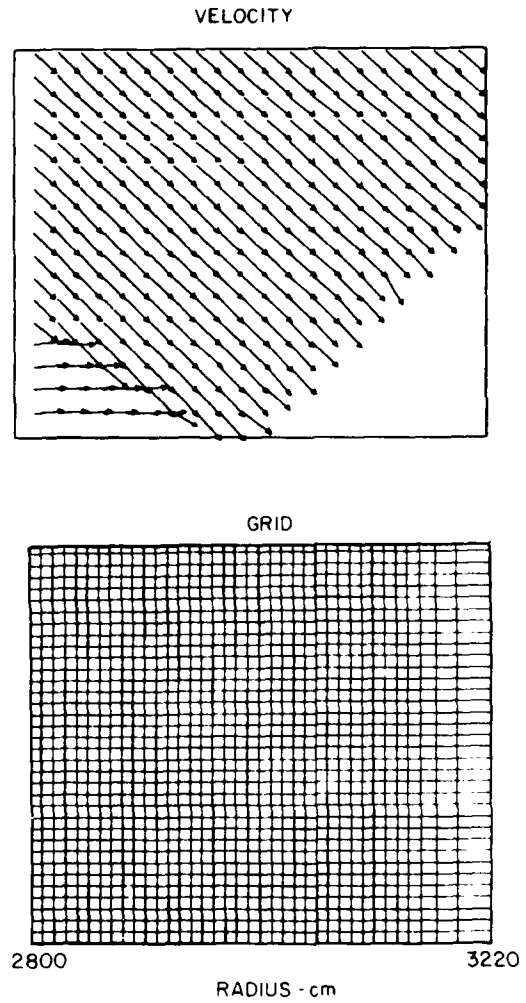
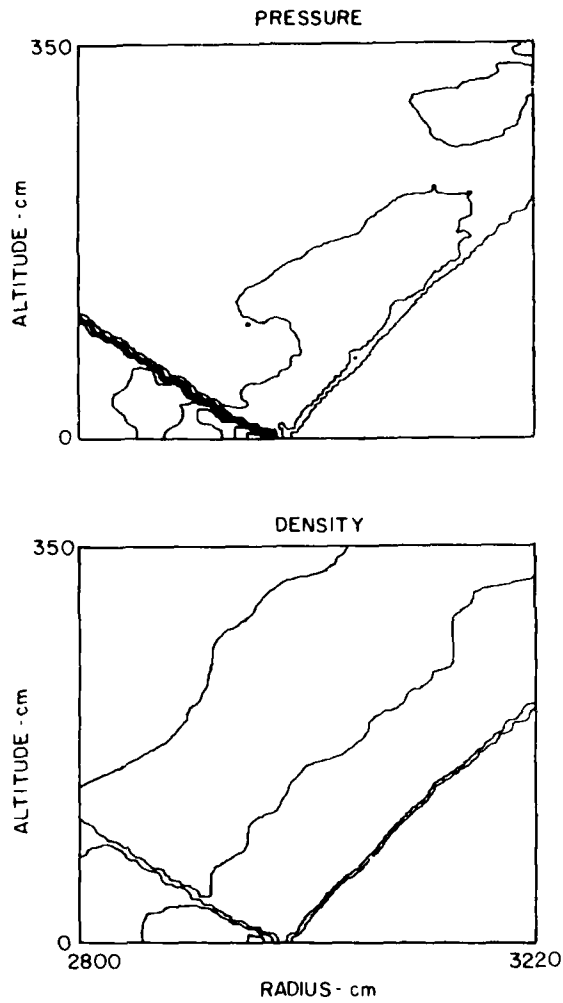
CYCLE = 4600



1 kt AT 104 ft HOB

TIME = 4.99 msec

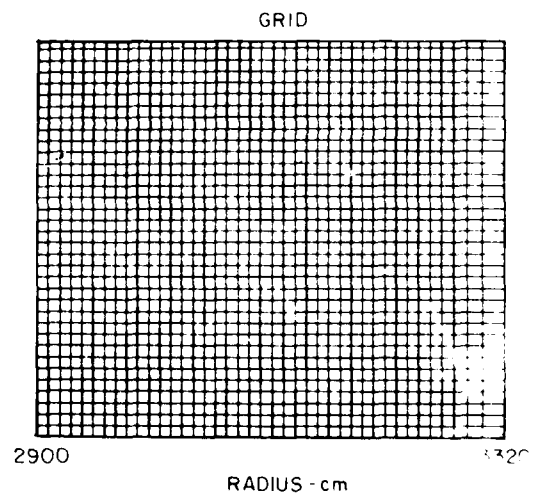
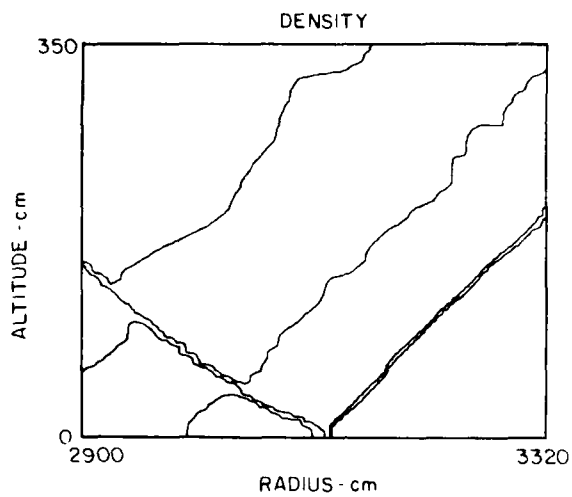
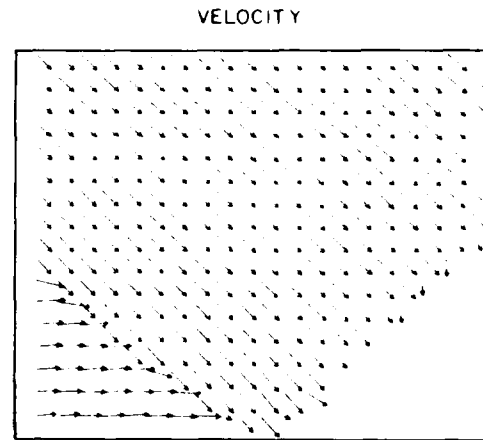
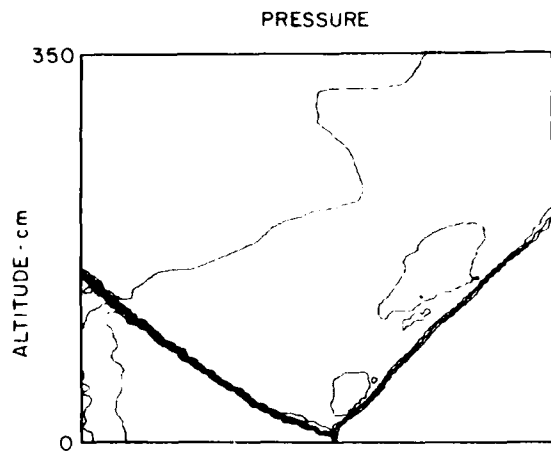
CYCLE = 5000



1 kt AT 104 ft HOB

TIME = 5.47 msec

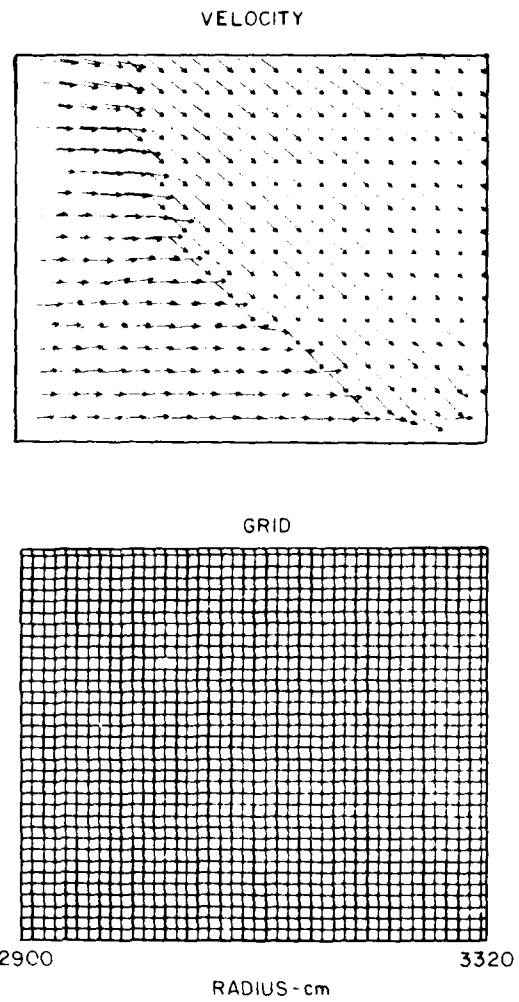
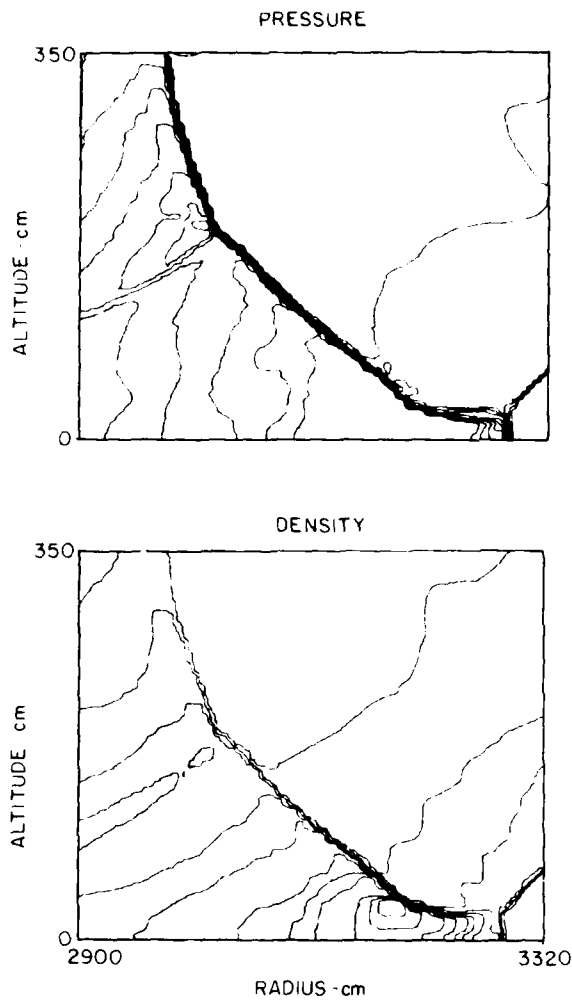
CYCLE = 5400



1 kt AT 104 ft HOB

TIME = 5.99 msec

CYCLE = 5800

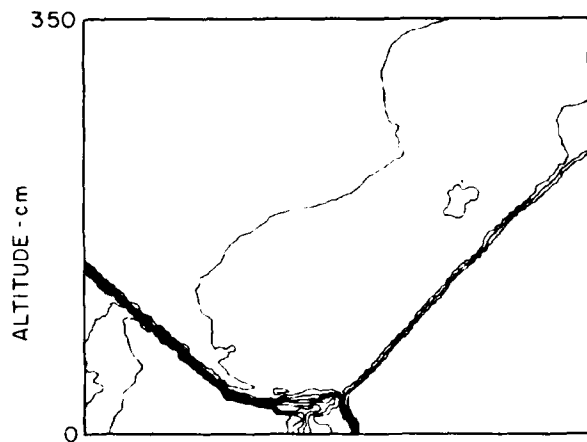


1 kt AT 104 ft HOB

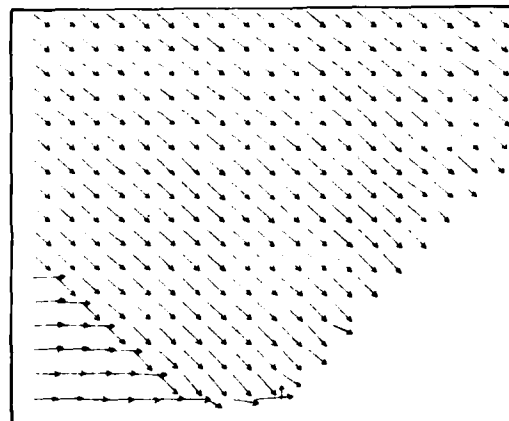
TIME = 6.26 msec

CYCLE = 6000

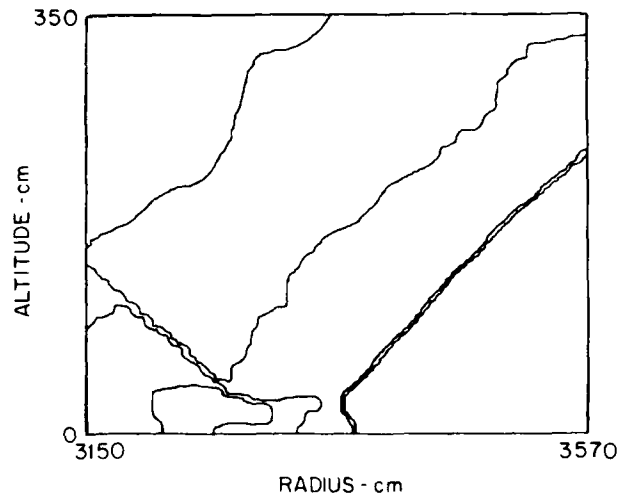
PRESSURE



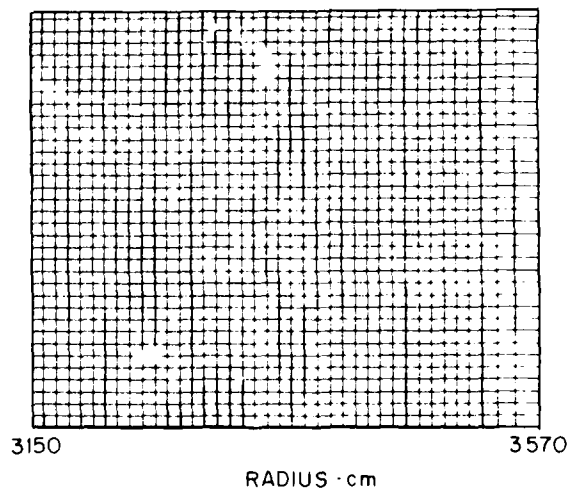
VELOCITY



DENSITY



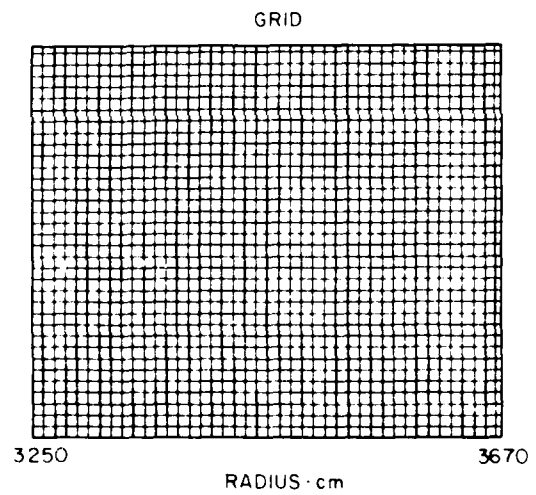
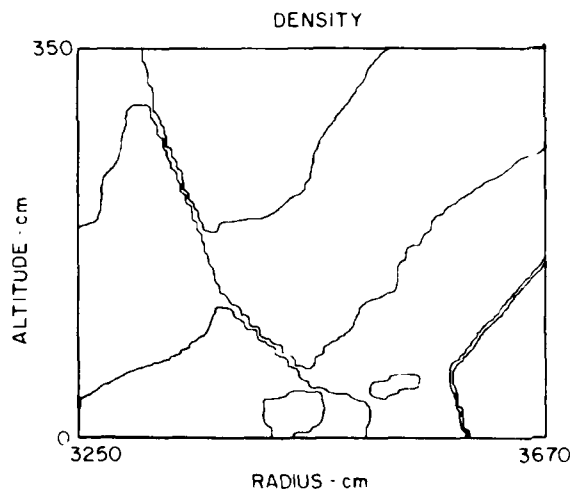
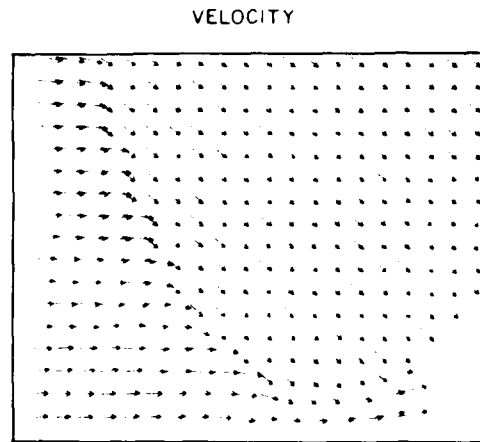
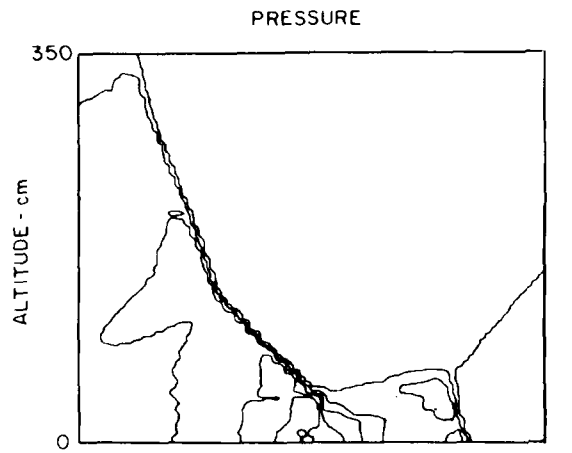
GRID



1 kt AT 104 ft HOB

TIME = 7.05 msec

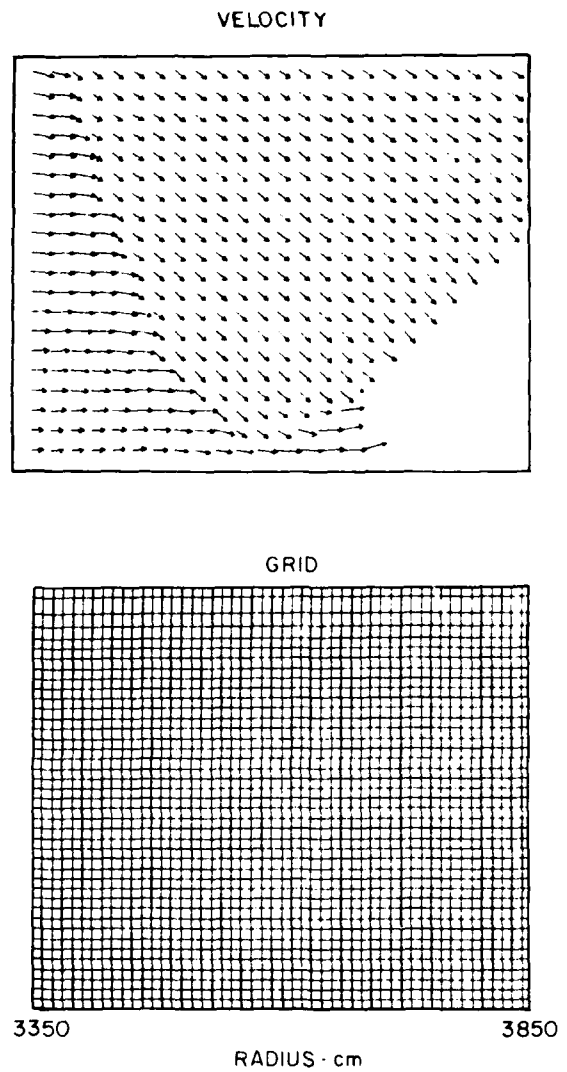
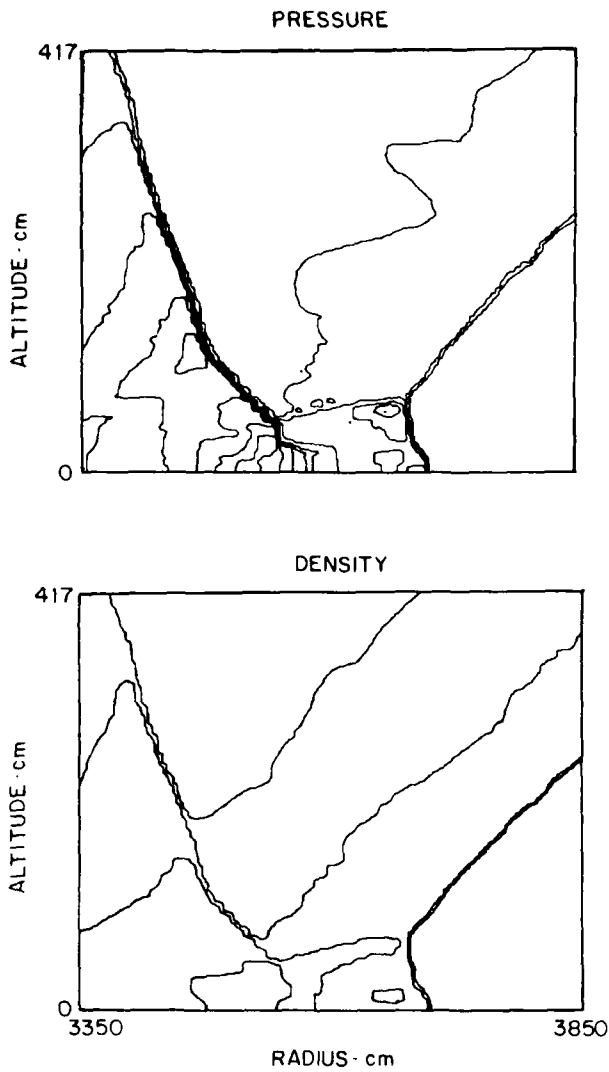
CYCLE = 6600



1kt AT 104 ft HOB

TIME = 7.39 msec

CYCLE = 6800

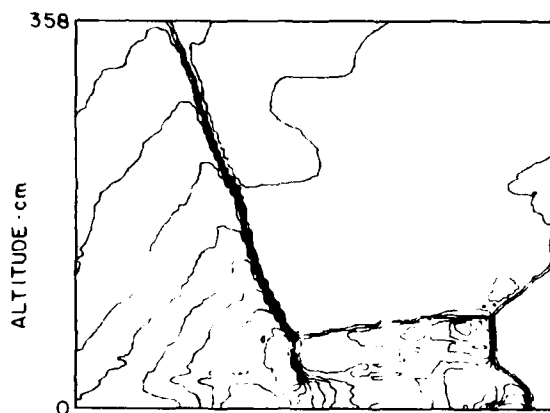


1 kt AT 104 ft HOB

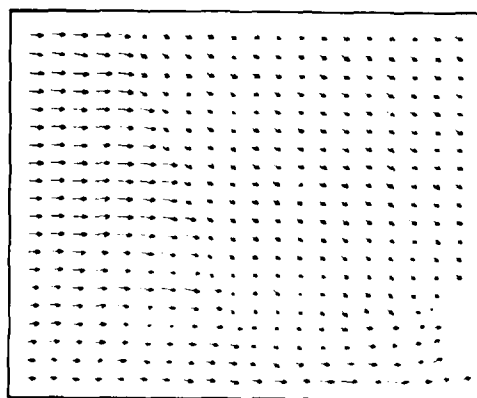
TIME = 8.28 msec

CYCLE = 7200

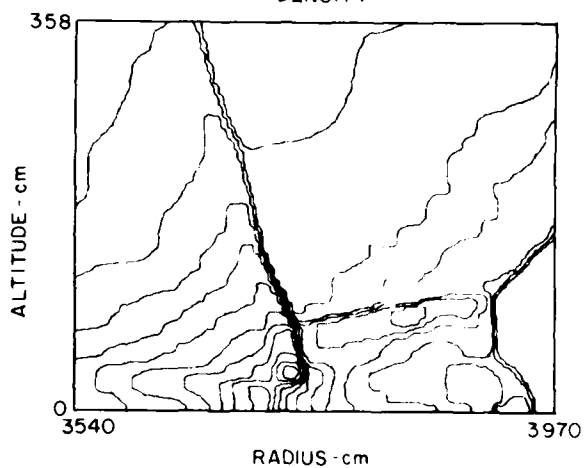
PRESSURE



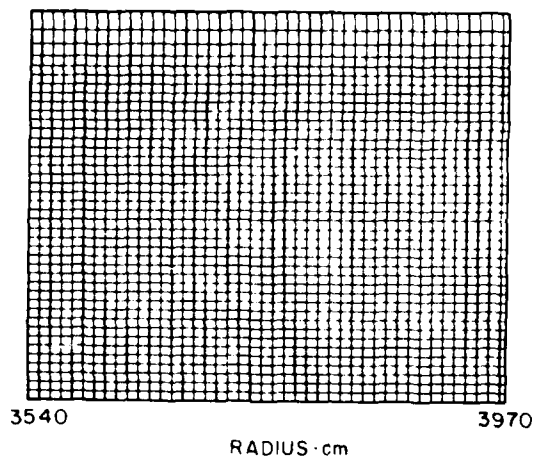
VELOCITY



DENSITY



GRID



DEPARTMENT OF ARMY

DIRECTOR
BMD ADVANCED TECHNOLOGY CENTER
DEPARTMENT OF THE ARMY
P O BOX 1500
HUNTSVILLE, AL 35807
OICY ATTN ATC-T
OICY ATTN ICRDASH-Y
OICY ATTN ATC-T

COMMANDER
BMD SYSTEMS COMMAND
DEPARTMENT OF THE ARMY
P O BOX 1500
HUNTSVILLE, AL 35807
OICY ATTN BMDSC-HA
OICY ATTN BMDSC-HA P DEKALB
OICY ATTN BMDSC-HA HURST
OICY ATTN BMDSC-HA WEBB

CHIEF OF ENGINEERS
DEPARTMENT OF THE ARMY
FORRESTAL BUILDING
WASHINGTON, DC 20314
OICY ATTN DAEN-ICE-D
OICY ATTN DAEN-RDL
OICY ATTN DAEN-XPF-T D REYNOLDS

DEP CH OF STAFF FOR OPS & PLANS
DEPARTMENT OF THE ARMY
WASHINGTON, DC 20310
OICY ATTN DAMC-MC

COMMANDER
HARRY DIAMOND LABORATORIES
DEPARTMENT OF THE ARMY
2300 POWDER MILL ROAD
ADELPHI, MD 20783
(CNWDI- INNER ENVELOPE: ATTN: DELHD-RBH FOR)
OICY ATTN DELHD-I-TL (TECH LIB)
OICY ATTN CHIEF DIV 20000

DEPARTMENT OF ARMY

COMMANDER
U S ARMY ARMAMENT MATERIAL READINESS COMMAND
ROCK ISLAND, IL 61202
OICV ATTN MA LIBRARY

DIRECTOR
U S ARMY BALLISTIC RESEARCH LABS
ABERDEEN PROVING GROUND, MD 21075
OICV ATTN DPBAR-BLV
OICV ATTN DPBAR-BLT J KEEFER
OICV ATTN DPBAR-TSP-S (TECH LIB)

COMMANDER AND DIRECTOR
U S ARMY CORP REGION RES ENGR LAB
P O BOX 282
HANOVER, NH 03755
OICV ATTN LIBRARY

COMMANDER
U S ARMY CONCEPTS ANALYSIS AGENCY
8120 WOODMONT AVENUE
BETHESDA, MD 20014
OICV ATTN C SSA-ADL (TECH LIB)

DIRECTOR
U S ARMY CONSTRUCTION ENGRG RES LAB
P O BOX 4005
CHAMPAIGN, IL 61820
OICV ATTN LIBRARY

COMMANDER
U S ARMY ENGINEER CENTER
FORT BELVOIR, VA 22060
OICV ATTN TECHNICAL LIBRARY
OICV ATTN ATZA

DEPARTMENT OF ARMY

DIVISION ENGINEER
U S ARMY ENGINEER DIV HUNTSVILLE
P O BOX 1600, WEST STATION
HUNTSVILLE, AL 35897
OICY ATTN HNDED SR
ATTN HNDED- FD /

DIRECTOR
U S ARMY ENGR WATERWAYS EXPR STATION
P O BOX 631
VICKSBURG, MS 39180
OICY ATTN J ZELASKO
OICY ATTN WESS J JACKSON
OICY ATTN J STRANGE
OICY ATTN WESS L INGRAM
OICY ATTN LIPPAPY
OICY ATTN WESSA W FLATHAU

COMMANDER
U S ARMY FOREIGN SCIENCE & TECH CTR
220 7TH STREET, NE
CHARLOTTESVILLE, VA 22901
OICY ATTN DRYST-SC

COMMANDER
U S ARMY MATERIAL & MECHANICAL RSCH CTR
WATERTOWN, MA 02172
(ADDRESS CNWDI: ATTN: DOCUMENT CONTROL FOR:)
OICY ATTN TECHNICAL LIBRARY
OICY ATTN DRYMP-TE R SHEA
OICY ATTN DRYMR J MESCALI

COMMANDER
U S ARMY MATERIAL DEV & READINESS CMD
5001 EISENHOWER AVENUE
ALEXANDRIA, VA 22304
OICY ATTN DRODE-D L FLYNN
OICY ATTN DRYM-TL (TECH LIB) UNCL ONLY

DEPARTMENT OF ARMY

COMMANDER
U S ARMY MISSILE COMMAND
REDSTONE ARSENAL, AL 35898
OICY ATTN PSIC
OICY ATTN DROMI-XS

COMMANDER
U S ARMY MOBILITY EQUIP REG CMO
FORT BELVOIR, VA 22060
(CONVICT TO ARMY MAT DEV & READINESS COMMAND)
OICY ATTN DROMI-WC (TECH LIB)

COMMANDER
U S ARMY NUCLEAR & CHEMICAL AGENCY
7500 BACKLICK ROAD
BUILDING 2073
SPRINGFIELD, VA 22150
(DESIRES ONLY 1 CY TO LIBRARY)
OICY ATTN J SIMMS
OICY ATTN LIBRARY

COMMANDANT
U S ARMY WAR COLLEGE
CAPTISLE BARRACKS, PA 17012
OICY ATTN LIBRARY

DEPARTMENT OF NAVY

COMMANDER

DAVID TAYLOR NAVAL SHIP R & D CTR
BETHESDA, MD 20084

(CNWDI ONLY ATTN MRS. M. BIRKHEAD CCDE 5815.6)
OICV ATTN CODE L42-3 (LIBRARY)

OFFICER-IN-CHARGE

NAVAL CIVIL ENGINEERING LABORATORY
PORT HUENEME, CA 93041

OICV ATTN CODE L53 J FORREST
OICV ATTN CODE L08A (LIBRARY)
OICV ATTN CODE L51 J CRAWFORD
OICV ATTN L51 P MURTHA

COMMANDER

NAVAL ELECTRONIC SYSTEMS COMMAND
WASHINGTON, DC 20360

OICV ATTN PMS 117-21

COMMANDER

NAVAL FACILITIES ENGINEERING COMMAND
WASHINGTON, DC 20390

OICV ATTN CODE 048

HEADQUARTERS

NAVAL MATERIAL COMMAND
WASHINGTON, DC 20360

OICV ATTN MAT OPT-22

COMMANDER

NAVAL OCEAN SYSTEMS CENTER
SAN DIEGO, CA 92152

OICV ATTN CODE 013 E COOPER
OICV ATTN CODE 4471 (TECH LIB)

DEPARTMENT OF NAVY

SUPERINTENDENT
NAVAL POSTGRADUATE SCHOOL
MONTEREY, CA 93940
(DESIRES NO CNWDI DOCUMENTS)
OICV ATTN CODE 1424 LIBRARY
OICV ATTN G LINDSAY

COMMANDING OFFICER
NAVAL RESEARCH LABORATORY
WASHINGTON, DC 20375
(RD & RD/N ATTN CODE 1221 FOR & FRD ATTN CODE 2628 FOR)
OICV ATTN CODE 4040 J BORIS
OICV ATTN CODE 2627 (TECH LIB)
OICV ATTN CODE 4040 D BOCK

COMMANDER
NAVAL SEA SYSTEMS COMMAND
WASHINGTON, DC 20362
OICV ATTN SEA-00653 (LIB)
OICV ATTN SEA-0351

OFFICER IN CHARGE
NAVAL SURFACE WEAPONS CENTER
WHITE OAK LABORATORY
SILVER SPRING, MD 20910
OICV ATTN P44 H CLAZ
OICV ATTN CODE F21
OICV ATTN CODE Y211 (TECH LIB)

COMMANDER
NAVAL SURFACE WEAPONS CENTER
DAHLGREN, VA 22448
OICV ATTN TECH LIBRARY & INFO SVCS BR

PRESIDENT
NAVAL WAR COLLEGE
NEWPORT, RI 02840
OICV ATTN CODE E-11 (TECH SERVICE)

DEPARTMENT OF NAVY

COMMANDER
NAVAL WEAPONS CENTER
CHINA LAKE, CA 93555
OICY ATTN CODE 3201 P CORDLE
OICY ATTN CODE 266 C AUSTIN
OICY ATTN CODE 223 (TECH LIB)

COMMANDING OFFICER
NAVAL WEAPONS EVALUATION FACILITY
KIRTLAND AIR FORCE BASE
ALBUQUERQUE, NM 87117
OICY ATTN R HUGHES
OICY ATTN CODE 10 (TECH LIB)

OFFICE OF NAVAL RESEARCH
ARLINGTON, VA 22217
OICY ATTN CODE 474 N PERRONE

OFFICE OF THE CHIEF OF NAVAL OPERATIONS
WASHINGTON, DC 20350
OICY ATTN OP 541
OICY ATTN OP 0356

DIRECTOR
STRATEGIC SYSTEMS PROJECT OFFICE
DEPARTMENT OF THE NAVY
WASHINGTON, DC 20376
OICY ATTN NSP-272
OICY ATTN NSP-43 (TECH LIB)

DEPARTMENT OF THE AIR FORCE

AIR FORCE GEOPHYSICS LABORATORY
HANSCOM AFB, MA 01731
OICY ATTN LHM K THOMPSON

AIR FORCE INSTITUTE OF TECHNOLOGY
AIR UNIVERSITY
WRIGHT-PATTERSON AFB, OH 45433
(DOES NOT DESIRE CLASSIFIED DOCUMENTS)
OICY ATTN LIBRARY

HEADQUARTERS
AIR FORCE SYSTEMS COMMAND
ANDREWS AFB, DC 20334
OICY ATTN DLWM
OICY ATTN DLW

AIR FORCE WEAPONS LABORATORY, AFSC
KIRTLAND AFB, NM 87117
OICY ATTN NTES-C R HENNY
OICY ATTN NTED-I
OICY ATTN NTED R MATAUCCI
OICY ATTN NTF M PLAMONDON
OICY ATTN NT D PAYTON
OICY ATTN NTED-A
OICY ATTN NTES-G
OICY ATTN SUL
OICY ATTN DEY
OICY ATTN NTES-S
OICY ATTN NTEC
OICY ATTN DEY

DIRECTOR
AIR UNIVERSITY LIBRARY
DEPARTMENT OF THE AIR FORCE
MAXWELL AFB, AL 36112
(DESIRES NO CNVDI)
OICY ATTN AUL-LSE

DEPARTMENT OF THE AIR FORCE

ASSISTANT CHIEF OF STAFF
INTELLIGENCE
DEPARTMENT OF THE AIR FORCE
WASHINGTON, DC 20330
OICY ATTN IN RM 4A932

ASSISTANT CHIEF OF STAFF
STUDIES & ANALYSES
DEPARTMENT OF THE AIR FORCE
WASHINGTON, DC 20330
OICY ATTN AF/SAMI (TECH LIB)

ASSISTANT SECRETARY OF THE AF
RESEARCH, DEVELOPMENT & LOGISTICS
DEPARTMENT OF THE AIR FORCE
WASHINGTON, DC 20330
OICY ATTN SAFALP/CEP FOR STRAT & SPACE SYS

BALLISTIC MISSILE OFFICE/IN
AIR FORCE SYSTEMS COMMAND
NORTON AFB, CA 92409
(MINUTEMAN)
OICY ATTN MNXXH G KALANSKY
OICY ATTN MNXXH M DELVECCHIO
OICY ATTN MNN W CPABTREE
OICY ATTN MNXXH D GAGE
OICY ATTN MNNX

DEPUTY CHIEF OF STAFF
RESEARCH, DEVELOPMENT, & ACQ
DEPARTMENT OF THE AIR FORCE
WASHINGTON, DC 20330
OICY ATTN AFROQI N ALEXANDROW
OICY ATTN AFROQI
OICY ATTN AFROQI

DEPARTMENT OF THE AIR FORCE

DEPUTY CHIEF OF STAFF
LOGISTICS & ENGINEERING
DEPARTMENT OF THE AIR FORCE
WASHINGTON, DC 20330
OICY ATTN LEFF

COMMANDER
FOREIGN TECHNOLOGY DIVISION, AFSC
WRIGHT-PATTERSON AFB, OH 45433
OICY ATTN NIIS LIBRARY

COMMANDER
ROYAL AIR DEVELOPMENT CENTER, AFSC
GRIFFISS AFB, NY 13441
(DESIRES NO CMMOT)
OICY ATTN TSLO

STRATEGIC AIR COMMAND
DEPARTMENT OF THE AIR FORCE
OFFUTT AFB, NE 68112
OICY ATTN NRI-STINCO LIBRARY
OICY ATTN XPES
OICY ATTN INT J MCKINNEY

VELA SEISMOLOGICAL CENTER
312 MONTGOMERY STREET
ALEXANDRIA, VA 22314
OICY ATTN G HILLPICH

DEPARTMENT OF ENERGY/DOE CONTRACTORS

DEPARTMENT OF ENERGY
ALBUQUERQUE OPERATIONS OFFICE
P O BOX 5400
ALBUQUERQUE, NM 87115
OICY ATTN CTID

DEPARTMENT OF ENERGY
WASHINGTON, DC 20545
OICY ATTN CMA/ROBT

DEPARTMENT OF ENERGY
NEVADA OPERATIONS OFFICE
P O BOX 14100
LAS VEGAS, NV 89114
OICY ATTN MAIL & RECORDS FOR TECHNICAL LIBRARY

LAWRENCE LIVERMORE NATIONAL LAB
P O BOX 808
LIVERMORE, CA 94550
OICY ATTN L-20 R DONG
OICY ATTN L-205 J HEAPST (CLASS L-203)
OICY ATTN L-90 D MORRIS (CLASS L-504)
OICY ATTN L-7 J KAHN
OICY ATTN D GLENN
OICY ATTN L 437 R SCHECK
OICY ATTN TECHNICAL INFO DEPT. LIBRARY
OICY ATTN L-200 T BLIKOVICH

LOS ALAMOS NATIONAL SCIENTIFIC LAB
MAIL STATION 5000
P O BOX 1663
LOS ALAMOS, NM 87545
(CLASSIFIED ONLY TO MAIL STATION 5000)
OICY ATTN P WHITTAKER
~~OICY ATTN P SCIDWELL~~
OICY ATTN C KELLER
OICY ATTN ~~M STANFORD~~ M.T. Stanford
OICY ATTN MS 364 (CLASS REPORTS LIB)
OICY ATTN E JONES

DEPARTMENT OF ENERGY/DOE CONTRACTORS

LOVELACE BIOMEDICAL &
ENVIRONMENTAL RESEARCH INSTITUTE, INC.
P O BOX 5990
ALBUQUERQUE, NM 87115
OICY ATTN R JONES (UNCL ONLY)

OAK RIDGE NATIONAL LABORATORY
NUCLEAR DIVISION
X-10 LAB RECORDS DIVISION
P O BOX X
OAK RIDGE, TN 37830
OICY ATTN CIVIL DEF RES PROJ
OICY ATTN CENTRAL RESEARCH LIBRARY

SANDIA LABORATORIES
LIVERMORE LABORATORY
P O BOX 969
LIVERMORE, CA 94550

SANDIA NATIONAL LAB
P O BOX 5800
ALBUQUERQUE, NM 87185
(ALL CLASS ATTN SEC CONTROL OFC FOR)
OICY ATTN A CHABAN
OICY ATTN L HILL
OICY ATTN ORG 1250 W BROWN
OICY ATTN A CHABIA
OICY ATTN W ROBERTY
OICY ATTN 3141
OICY ATTN L VORTMAN
OICY ATTN J. Benister

Revised

DEPARTMENT OF DEFENSE CONTRACTORS

ACUREX CORP.
485 CLYDE AVENUE
MOUNTAIN VIEW, CA 94042
OICY ATTN C WOLF

AEROSPACE CORP.
P O BOX 92957
LOS ANGELES, CA 90009
OICY ATTN H WIRELS
OICY ATTN TECHNICAL INFORMATION SERVICES

AGBABIAN ASSOCIATES
250 N NASH STREET
EL SEGUNDO, CA 90245
OICY ATTN M AGBABIAN

ANALYTIC SERVICES, INC.
400 ARMY-NAVY DRIVE
ARLINGTON, VA 22202
OICY ATTN G HESSELBACHER

APPLIED RESEARCH ASSOCIATES, INC
2601 WYOMING BLVD NE SUITE F-1
ALBUQUERQUE, NM 87112
OICY ATTN J PRATTEN
OICY ATTN N HIGGINS

APPLIED THEORY, INC.
1010 WESTWOOD BLVD
LOS ANGELES, CA 90024
(2 CYS IF UNCLASS OR 1 CY IF CLASS)
OICY ATTN J TRULLIO

DEPARTMENT OF DEFENSE CONTRACTORS

ARTEC ASSOCIATES, INC.
26046 EDEN LANDING ROAD
HAYWARD, CA 94545
OICY ATTN S GILL

ASTRON RESEARCH & ENGINEERING
1901 OLD MIDDLEFIELD WAY #15
MOUNTAIN VIEW, CA 94043
OICY ATTN J HUNTINGTON

AVCO RESEARCH & SYSTEMS GROUP
201 LOWELL STREET
WILMINGTON, MA 01887
OICY ATTN LIBRARY A630

BDM CORP.
7915 JONES BRANCH DRIVE
MCLEAN, VA 22102
OICY ATTN A LAVAGNINO
OICY ATTN T NEIGHROPS
OICY ATTN CORPORATE LIBRARY

BDM CORP.
P O BOX 9274
ALBUQUERQUE, NM 87119
OICY ATTN R HENSLEY

BOEING CO.
P O BOX 3707
SEATTLE, WA 98124
OICY ATTN S STRACK
OICY ATTN AFROSPACE LIBRARY
OICY ATTN M/S 42/37 P CARLSON

DEPARTMENT OF DEFENSE CONTRACTORS

CALIFORNIA RESEARCH & TECHNOLOGY, INC.
6269 VARIEL AVENUE
WOODLAND HILLS, CA 91367
OICV ATTN LIBRARY
OICV ATTN K KREYENHAGEN
OICV ATTN M ROSENBLATT

CALIFORNIA RESEARCH & TECHNOLOGY, INC.
4049 FIRST STREET
LIVERMORE, CA 94550
OICV ATTN D ORPHAL

CALSPAN CORP.
P O BOX 400
BUFFALO, NY 14225
OICV ATTN LIBRARY

DENVER, UNIVERSITY OF
COLORADO SEMINARY
DENVER RESEARCH INSTITUTE
P O BOX 10127
DENVER, CO 80210
(ONLY 1 COPY OF CLASS RPTS)
OICV ATTN SEC OFFICER FOR J WISOTSKI

EG&G WASH. ANALYTICAL SVCS CTR, INC.
P O BOX 1021P
ALBUQUERQUE, NM 87114
OICV ATTN LIBRARY

DEPARTMENT OF DEFENSE CONTRACTORS

ERIC H. WANG
CIVIL ENGINEERING PSCH FAC
UNIVERSITY OF NEW MEXICO
UNIVERSITY STATION
P O BOX 25
ALBUQUERQUE, NM 87131
OICV ATTN J LAMB
OICV ATTN P LEODE
OICV ATTN N BAUM
OICV ATTN J KOVARNA

GARD, INC.
7449 N NATCHEZ AVENUE
NILES, IL 60648
OICV ATTN G NEIGHARDT (INCL ONLY)

GENERAL ELECTRIC CO.
SPACE DIVISION
VALLEY FORGE SPACE CENTER
P O BOX 9555
PHILADELPHIA, PA 19101
OICV ATTN M BOPTNER

GENERAL RESEARCH CORP.
SANTA BARBARA DIVISION
P O BOX 6770
SANTA BARBARA, CA 93111
OICV ATTN TIC

H-TECH LABS, INC.
P O BOX 1686
SANTA MONICA, CA 90406
OICV ATTN B HARTENDALM

DEPARTMENT OF DEFENSE CONTRACTORS

HORIZONS TECHNOLOGY, INC.
7830 CLAIEMONT MESA BLVD
SAN DIEGO, CA 92111
OICY ATTN R KRUGER

IIT RESEARCH INSTITUTE
10 W 35TH STREET
CHICAGO, IL 60616
OICY ATTN R FELCH
OICY ATTN M JOHNSON
OICY ATTN DOCUMENTS LIBRARY

INFORMATION SCIENCE, INC.
123 W PADRE STREET
SANTA BARBARA, CA 93105
OICY ATTN W DUDZIAK

INSTITUTE FOR DEFENSE ANALYSIS
400 ARMY-NAVY DRIVE
ARLINGTON, VA 22202
OICY ATTN CLASSIFIED LIBRARY

J D HALTIWANGER CONSULT ENG SVCS
RM 106A CIVIL ENGINEERING BLDG
208 N ROMINE STREET
URBANA, IL 61801
OICY ATTN W HALL

J. H. WIGGINS CO., INC.
1650 S PACIFIC COAST HIGHWAY
REDONDO BEACH, CA 90277
OICY ATTN J COLLINS

DEPARTMENT OF DEFENSE CONTRACTORS

KAMAN AVIDYNE
83 SECOND AVENUE
NORTHWEST INDUSTRIAL PARK
BURLINGTON, MA 01203
OICY ATTN P RLETENIK
OICY ATTN LIBRARY
OICY ATTN M HOBBS
OICY ATTN E CRISCIONE

KAMAN SCIENCES CORP.
P O BOX 7463
COLORADO SPRINGS, CO 80933
OICY ATTN D SACHS
OICY ATTN F SHELTON
OICY ATTN LIBRARY

KAMAN TEMPO
816 STATE STREET (P O DRAWER 00)
SANTA BARRARA, CA 92102
OICY ATTN DASIAC

LOCKHEED MISSILES & SPACE CO., INC.
P O BOX 504
SUNNYVALE, CA 94086
OICY ATTN J WEISNER
OICY ATTN TIC-LIBRARY

MARTIN MARIETTA CORP.
P O BOX 5837
ORLANDO, FL 32855
OICY ATTN G FCTIEC

MARTIN MARIETTA CORP.
P O BOX 179
DENVER, CO 80201
OICY ATTN G FREYER

DEPARTMENT OF DEFENSE CONTRACTORS

MCDONNELL DOUGLAS CORP.
5301 BOLSA AVENUE
HUNTINGTON BEACH, CA 92647
OICY ATTN H HERDMAN
OICY ATTN R HALPRIN
OICY ATTN D DEAN

MCDONNELL DOUGLAS CORP.
3855 LAKEWOOD BOULEVARD
LONG BEACH, CA 90846
OICY ATTN M POTTER

MERRITT CASES, INC.
P O BOX 1206
REDLANDS, CA 92373
OICY ATTN J MERRITT
OICY ATTN LIPARY

METEOROLOGY RESEARCH, INC.
464 W WOODBURY ROAD
ALTADENA, CA 91001
OICY ATTN W GREEN

MISSION RESEARCH CORP.
P O DRAWER 719
SANTA BARBARA, CA 93102
(ALL CLASS: ATTN: SEC OFC FOR)
OICY ATTN G LONGMIRE
OICY ATTN G MCCARTER

PACIFIC-SIERRA RESEARCH CORP.
1456 CLOVERFIELD BLVD
SANTA MONICA, CA 90404
OICY ATTN H BRODE

DEPARTMENT OF DEFENSE CONTRACTORS

PACIFIC-SIERPA RESEARCH CORP.
WASHINGTON OPERATIONS
1401 WILSON BLVD
SUITE 1100
ARLINGTON, VA 22209
OICY ATTN D GORMLEY

PACIFICA TECHNOLOGY
P O BOX 149
DEL MAR, CA 92014
OICY ATTN R BJORK
OICY ATTN G KENT
OICY ATTN TECH LIBRARY

PATEL ENTERPRISES, INC.
P O BOX 3531
HUNTSVILLE, AL 35910
OICY ATTN M PATEL

PHYSICS INTERNATIONAL CO.
2700 MERCED STREET
SAN LEANDRO, CA 94577
OICY ATTN L BEHRMANN
OICY ATTN TECHNICAL LIBRARY
OICY ATTN F MOORE
OICY ATTN J THOMSEN
OICY ATTN F SAUER

R & D ASSOCIATES
P O BOX 9695
MARINA DEL REY, CA 90291
OICY ATTN R BORT
OICY ATTN A KIMH
OICY ATTN J LEXIS
OICY ATTN W WRIGHT
OICY ATTN J CARPENTER
OICY ATTN TECHNICAL INFORMATION CENTER

DEPARTMENT OF DEFENSE CONTRACTORS

PAND CORP.
1700 MAIN STREET
SANTA MONICA, CA 90406
OICV ATTN C MCM

SCIENCE APPLICATIONS, INC
RADIATION INSTRUMENTATION DIV
4615 HAWKINS, NE
ALBUQUERQUE, NM 87109
OICV ATTN J DISCH

SCIENCE APPLICATIONS, INC.
P O BOX 2351
LA JOLLA, CA 92039
OICV ATTN H WILSON
OICV ATTN TECHNICAL LIBRARY
OICV ATTN R SCHLAUG

SCIENCE APPLICATIONS, INC.
101 CONTINENTAL BLVD
FL SEGUNDO, CA 90245
OICV ATTN J HOVE

SCIENCE APPLICATIONS, INC.
2450 WASHINGTON AVENUE
SAN LEANDRO, CA 94577
OICV ATTN D BERNSTEIN
OICV ATTN D MAXWELL

SCIENCE APPLICATIONS, INC.
P O BOX 1303
MCLEAN, VA 22102
OICV ATTN J COCKAYNE
OICV ATTN B CHAMBERS III
OICV ATTN M KNASEL
OICV ATTN W LAYSON
OICV ATTN R SIEVERS

DEPARTMENT OF DEFENSE CONTRACTORS

SOUTHWEST RESEARCH INSTITUTE
P O DRAWER 28510
SAN ANTONIO, TX 78284
OICY ATTN A WENZEL
OICY ATTN W BAKER

SRI INTERNATIONAL
333 PAVENSWOOD AVENUE
MENLO PARK, CA 94025
OICY ATTN G ABRAHAMSON
OICY ATTN LIBRARY
OICY ATTN J COLTON

SYSTEMS, SCIENCE & SOFTWARE INC
P O BOX 8243
ALBUQUERQUE NM 87198
OICY ATTN C NEEDHAM

SYSTEMS, SCIENCE & SOFTWARE, INC.
P O BOX 1620
LA JOLLA, CA 92038
OICY ATTN J PARTHEL
OICY ATTN T RINEY
OICY ATTN D GRINE
OICY ATTN LIBRARY
OICY ATTN C HASTING
OICY ATTN K PYATT
OICY ATTN C DISMUKES
OICY ATTN T CHERRY

SYSTEMS, SCIENCE & SOFTWARE, INC.
11900 SUNRISE VALLEY DRIVE
RESTON, VA 22091
OICY ATTN J MURPHY

DEPARTMENT OF DEFENSE CONTRACTORS

TELEDYNE BROWN ENGINEERING
CUMMINGS RESEARCH PARK
HUNTSVILLE, AL 35897
OICY ATTN J RAVENSCRAFT
OICY ATTN J MCSWAIN

TERPA TEK, INC.
420 WAKARA WAY
SALT LAKE CITY, UT 84108
OICY ATTN A ABUHI-SAYED
OICY ATTN LIBRARY
OICY ATTN A JONES
OICY ATTN S GREEN

TETRA TECH, INC.
630 N POSEMEAD BLVD
PASADENA, CA 91107
OICY ATTN L HWANG

TRW DEFENSE & SPACE SYS GROUP
ONE SPACE PARK
REDONDO BEACH, CA 90278
OICY ATTN N LIPNER
OICY ATTN TECHNICAL INFORMATION CENTER
OICY ATTN T MAZZOLA

TRW DEFENSE & SPACE SYS GROUP
P O BOX 1310
SAN BERNARDINO, CA 92402
OICY ATTN G HULCHER
OICY ATTN P DAI
OICY ATTN E WONG

DEPARTMENT OF DEFENSE CONTRACTORS

UNIVERSAL ANALYTICS, INC.
7740 W MANCHESTER BLVD
PLAYA DEL REY, CA 90291
OICY ATTN E FIELD

WEIDLINGER ASSOC., CONSULTING ENGINEERS
110 E 59TH STREET
NEW YORK, NY 10022
OICY ATTN I SANDLER
OICY ATTN M PARDN

WEIDLINGER ASSOC., CONSULTING ENGINEERS
3000 SAND HILL ROAD
MENLO PARK, CA 94025
OICY ATTN J ISENBERG

*Chief Scientist
Naval Research Laboratory
Laboratory for Computational Physics
Code 4040
Washington, D.C. 20375
100cy Attn J. Boris*

DEPARTMENT OF DEFENSE

ASSISTANT TO THE SECRETARY OF DEFENSE
(ATOMIC ENERGY)

WASHINGTON, DC 20301

OICY ATTN EXECUTIVE ASSISTANT

DIRECTOR

DEFENSE COMMUNICATIONS AGENCY

WASHINGTON, DC 20305

(ADD CNMCI: ATTN CODE 240 FOR)

OICY ATTN CODE 570 F LIPP

DIRECTOR

DEFENSE INTELLIGENCE AGENCY

WASHINGTON, DC 20301

OICY ATTN RDS-2A (TECH LIP)

OICY ATTN DB 4N

OICY ATTN DT 1C

OICY ATTN DT-2

OICY ATTN DB 4C F DEAPRELL

DIRECTOR

DEFENSE NUCLEAR AGENCY

WASHINGTON, DC 20305

O2CY ATTN SPSS

O1CY ATTN SPSS G ULLRICH

O1CY ATTN SPSS T DEEVY

O4CY ATTN TITL

DEFENSE TECHNICAL INFORMATION CENTER

CAMERON STATION

ALEXANDRIA, VA 22314

(12 IF OPEN PUB, OTHERWISE 2 NO MAINTFL)

2CY ATTN OC

CHAIRMAN

DEPARTMENT OF DEFENSE EXPLO SAFETY BOARD

HOFFMAN BLDG 1, PM 856-C

2461 EISENHOWER AVENUE

ALEXANDRIA, VA 22301

OICY ATTN CHAIRMAN

DEPARTMENT OF DEFENSE

COMMANDER
FIELD COMMAND
DEFENSE NUCLEAR AGENCY
KIRTLAND AFB, NM 87115
OICY ATTN FCTMOR
OICY ATTN FCT
OICY ATTN FCPR
OICY ATTN FCTT

CHIEF
FIELD COMMAND
DEFENSE NUCLEAR AGENCY
LIVERMORE BRANCH
P O BOX 808 L-317
LIVERMORE, CA 94550
OICY ATTN FCPRL

DIRECTOR
JOINT STRAT TGT PLANNING STAFF
OFFUTT AFB
OMAHA, NB 68113
OICY ATTN JLA
OICY ATTN DOXT
OICY ATTN XPFS
OICY ATTN NRI-STINFO LIBRARY
OICY ATTN JLTW-2

COMMANDANT
NATO SCHOOL (SHAPE)
APO NEW YORK 09172
OICY ATTN U S DOCUMENTS OFFICER

UNDER SECY OF DEF FOR RSCH & ENGRG
DEPARTMENT OF DEFENSE
WASHINGTON, DC 20301
OICY ATTN STRATEGIC & SPACE SYS (CS) RM 3F129

OTHER GOVERNMENT

CENTRAL INTELLIGENCE AGENCY
WASHINGTON, DC 20505
OICV ATTN OSWP/NEC

DEPARTMENT OF THE INTERIOR
BUREAU OF MINES
BLDG 20, DENVER FEDERAL CENTER
DENVER, CO 80225
(UNCL ONLY)
OICV ATTN TECH LIP (UNCL ONLY)

DIRECTOR
FEDERAL EMERGENCY MANAGEMENT AGENCY
NATIONAL SEC OFC MITIGATION & RSCH
1725 I STREET, NW
WASHINGTON, DC 20472
(ALL CLASS ATTN BLOS DOC CONTROL FOR)
OICV ATTN MITIGATION & RSCH DIV

